BANANAS AND BANANA SPLITS: A PARAMETRIC DEGENERACY IN THE HOPF BIFURCATION FOR MAPS

BRUCE B. PECKHAM *, CHRISTOS E. FROUZAKIS †, AND IOANNIS G. KEVREKIDIS ‡

Draft: August 5, 1993

Abstract. The set of Hopf bifurcations for a two-parameter family of maps is typically a curve in the parameter plane. The side of the curve on which the invariant circle exists is further divided by horn-shaped resonance regions, each region corresponding to maps having a periodic orbit of a certain period. With the presence of a parametric degeneracy, the resonance regions sometimes take the form of closed "bananas", instead of open-ended horns. We investigate this local codimension-two bifurcation, emphasizing resonance regions as projections to the parameter plane of surfaces in phase $\times$ parameter space. We present scenarios where the degeneracy occurs "naturally", and illustrate them through an adaptive control application. We also discuss more global implications of the local study.

Key words. Hopf bifurcation, resonance, Arnold horns, parametric degeneracy

AMS subject classifications. 58F14, 58F40

1. Introduction. When a fixed point for a map of $\mathbf{R}^n, n \geq 2$, has a complex conjugate pair of eigenvalues on the unit circle, we expect it to undergo a Hopf (also called Neimark–Sacker) bifurcation under perturbation. In a typical two-parameter family containing such a point, there is a Hopf bifurcation curve in the parameter plane which separates maps with an attracting fixed point from those with a repelling fixed point. The change in stability of the fixed point across the Hopf curve is accompanied, except possibly near the "strong resonances", by the birth of an invariant topological circle from the fixed point. The side of the Hopf curve on which the invariant circle exists, as well as its stability, is determined by the relationship between the parameters, the linear terms and some nonlinear terms in the family of maps. Excepting again parameter values near strong resonances, it is known that all local recurrence is restricted to the fixed point and to the invariant circle, when the latter exists.

On the side of the Hopf curve without the invariant circle, all nearby maps are locally topologically equivalent. On the side with the invariant curve, however, the parameter space must be further subdivided because, restricted to the invariant circle, we expect the rotation number of the maps, a topological invariant, to change with the parameters. From circle map theory we know that the existence of a reduced rational rotation number p/q implies the existence of at least one least-period-q orbit, so we concentrate in this paper on determining the location in phase $\times$ parameter space where periodic orbits of certain period exist. Such sets are called "period-q resonance surfaces", or "p/q resonance surfaces" if we wish to identify the rotation number of the

* Department of Mathematics and Statistics, University of Minnesota at Duluth, Duluth, Minnesota 55812. Work was partially supported by National Science Foundation grant DMS 9020220.

† Department of Chemical Engineering, Princeton University, Princeton, NJ 08544. Present address, Institut für Energietechnik, ETH Zentrum, CH-8092, Zürich, Switzerland. Work was partially supported by DARPA/ONR grant # N00014-91-J-1850.

‡ Department of Chemical Engineering, Princeton University, Princeton, NJ 08544. Work was partially supported by DARPA/ONR grant # N00014-91-J-1850. A David and Lucile Packard Foundation Fellowship is also gratefully acknowledged.

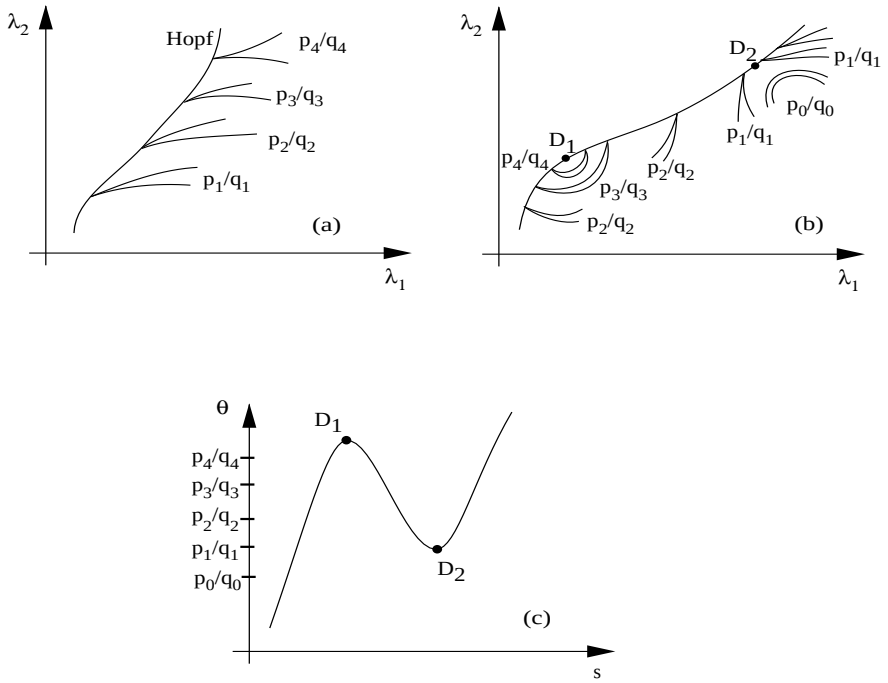

FIG. 1. *Typical Hopf bifurcations: (a) Parameter plane without angular degeneracies (b) Parameter plane with two angular degeneracies (at D_1 and D_2) (c) Angle θ of fixed-point eigenvalue vs. arc length s along the Hopf curve in (b).*

period-q orbit. Their projections to parameter space are called "period-q resonance regions", or "p/q resonance regions", or "(Arnold) resonance horns" if we wish to suggest their shape. They are also called "phase locking regions" or "entrainment regions", both names having originated in the context of "Poincarè maps" of two frequency flows on a torus; in this case, regions of constant frequency ratio for the flow correspond to regions of existence of a certain periodic orbit for the map.

It is known that a period-q resonance region typically "opens out" from every point on the Hopf curve for which the fixed point has an eigenvalue of $e^{2\pi ip/q}$, p/q any rational with $q \geq 5$, as suggested in Figure 1a. In order to ensure that a specific resonance region opens in the horn–shaped manner suggested by that figure, several nondegeneracy conditions must be satisfied. Some nondegeneracy conditions pertain only to the phase variables, others include reference to the parameters as well. The failure of any one of the nondegeneracy conditions to hold results in a "degenerate" Hopf bifurcation. Of specific interest to us is the following nondegeneracy condition with respect to the parameters: it is usually assumed that the argument of eigenvalues of the fixed point varies monotonically along the Hopf curve. When the argument *fails* to vary monotonically we say the Hopf bifurcation has an **angular degeneracy**. In this case, the nearby Arnold resonance regions can appear locally in shapes such as closed "bananas" rather than as the open horns of Figure 1a. Figure 1b suggests a possible scenario for resonance regions near the Hopf bifurcation curve. The Hopf points with angular degeneracies are at D_1, a "banana" point, and at D_2, a "banana-split" point.

To emphasize the non-monotonicity at the points with angular degeneracies, we show in Figure 1c the argument of one of the eigenvalues of the neutral fixed point

as a function of arclength, s, along the Hopf bifurcation curve of Figure 1b. The argument fails to vary monotonically through points D_1 and D_2.

To be more precise, we make the following definition. Unless otherwise noted, we assume throughout the paper that we are dealing with a k-parameter family of functions $\mathbf{F}_\mu : \mathbf{R}^2 \to \mathbf{R}^2, \boldsymbol{\mu} \in \mathbf{R}^k$, which is C^∞ as a function from $\mathbf{R}^2 \times \mathbf{R}^k \to \mathbf{R}^2$. We will be mostly interested in two-parameter families ($k = 2$).

Definition: Let $\mathbf{F}_\mu$ be a family of smooth maps of the plane with the following properties:

1. A map in the family has a fixed point:

$$\mathbf{F}_{\mu_0}(\mathbf{x}_0) = \mathbf{x}_0$$

2. The fixed point is "nonhyperbolic", with complex conjugate eigenvalues on the unit circle:

$$D\mathbf{F}_{\mu_0}(\mathbf{x}_0) \text{ has eigenvalues } e^{\pm 2\pi i\omega_0}$$

where $\omega_0 \in \mathbf{R}$, but $2\omega_0 \notin \mathbf{Z}$ to ensure that the eigenvalues in a neighborhood of the bifurcation point are complex.
Then $(\mathbf{x}_0, \boldsymbol{\mu}_0)$ is a **Hopf bifurcation point** for the family $\mathbf{F}_\mu$.

The implicit function theorem guarantees that there exist unique fixed points near $\mathbf{x}_0$ for maps $\mathbf{F}_\mu$ corresponding to parameter values $\boldsymbol{\mu}$ near $\boldsymbol{\mu}_0$. The fixed points can be described by a C^∞ function $\mathbf{x} = \mathbf{x}(\boldsymbol{\mu})$ satisfying $\mathbf{x}(\boldsymbol{\mu}_0) = \mathbf{x}_0$. The eigenvalues of the nearby fixed point $\mathbf{x}(\boldsymbol{\mu})$ can be written as $\lambda_\pm = \lambda_\pm(\boldsymbol{\mu}) = \lambda_\pm(\mathbf{x}(\boldsymbol{\mu})) = e^{\rho(\mu)\pm i(2\pi\omega_0+\alpha(\mu))}$. This defines $\rho(\boldsymbol{\mu})$ uniquely, and $\alpha(\boldsymbol{\mu})$ uniquely, once a choice of ω_0 has been fixed, as C^∞ functions which must satisfy $\rho(\boldsymbol{\mu}_0) = 0, \alpha(\boldsymbol{\mu}_0) = 0$.

It is customary to study the Hopf bifurcation by making a change of parameters to (ρ, α) from the original parameters $\boldsymbol{\mu}$. This is possible whenever $\nabla_\mu\rho(\boldsymbol{\mu}_0)$ and $\nabla_\mu\alpha(\boldsymbol{\mu}_0)$ are linearly independent vectors.

Definition: The point $(\mathbf{x}_0, \boldsymbol{\mu}_0)$ is a **Hopf bifurcation point with a parametric degeneracy** if the vectors $\nabla_\mu\rho(\boldsymbol{\mu}_0)$ and $\nabla_\mu\alpha(\boldsymbol{\mu}_0)$ are *not* linearly independent.

Definition: A Hopf bifurcation point satisfies the **eigenvalue crossing condition** if

$$\nabla_\mu\rho(\boldsymbol{\mu}_0) \neq \mathbf{0}$$

Definition: We say $(\mathbf{x}_0, \boldsymbol{\mu}_0)$ is a **Hopf bifurcation point with an angular degeneracy** for the family $\mathbf{F}_\mu$ if it has a parametric degeneracy, but the eigenvalue crossing condition is satisfied.

When the eigenvalue crossing condition is satisfied, as it generically is in two-parameter families, the implicit function theorem guarantees the continuation of a Hopf bifurcation curve through $\boldsymbol{\mu}_0$ in the parameter plane. If we express the Hopf curve with arc length parametrization as $\boldsymbol{\mu} = \boldsymbol{\mu}(s)$ with $\mu(0) = \boldsymbol{\mu}_0$, it follows that $\rho(\boldsymbol{\mu}(s)) = 0$.

If we monitor the argument of the neutral eigenvalue of the fixed point along the Hopf curve, we see that having an angular degeneracy is equivalent to $\frac{d}{ds}\alpha(\boldsymbol{\mu}(s))|_{s=0} = 0$. This is why we call the degeneracy an *angular* degeneracy. An angular degeneracy

occurs either when $\nabla_\mu \alpha(\boldsymbol{\mu}_0)$ is nonzero but parallel to $\nabla_\mu \rho(\boldsymbol{\mu}_0)$ or when $\nabla_\mu \alpha(\mu_0) = \mathbf{0}$ (the latter being a nongeneric occurrence in two-parameter families).

We think of the Hopf bifurcation with an angular degeneracy as arising from two possible scenarios in applications. The first is easier to explain and understand: the "natural" parameters ($\boldsymbol{\mu}$ above) in an application are *not* related in a one-to-one fashion to the "universal unfolding" parameters of the modulus and angle of the eigenvalues of the associated fixed point for the corresponding map, or equivalent parameters such as $\rho(\boldsymbol{\mu})$ and $\alpha(\boldsymbol{\mu})$ defined above. The lack of injectivity causes singular points for the change of parameters from $\boldsymbol{\mu}$ to (ρ, α). Geometrically, we can think of curves of singular points as places we need to "fold" the natural parameter plane in order to place it on top of the corresponding points in the "universal" parameter plane. When the Hopf curve crosses such a fold curve in the natural parameter plane, we have an angular degeneracy. The description of the geometric "folding" of the parameter space is further detailed in subsection 2.4.

The other general scenario where an angular degeneracy arises is along a curve of "secondary" Hopf bifurcations in the two-dimensional parameter space. Although locally the same as an angular degeneracy on a primary Hopf curve, this case cannot be dismissed as merely an "unfortunate" choice of parameters because a "good" parameter choice is usually determined with respect to primary bifurcation phenomena. One codimension-two bifurcation point, a "Chenciner" or "transcritical Hopf" point, *requires* the existence of an infinity of angular degeneracies, each on its own secondary Hopf curve inside its own resonance region. It was in studying bifurcations near a Chenciner point, in fact, when we first became interested in the angular degeneracy we describe in this paper [Mc, Jo]. We discuss this scenario in more detail in Section 3. We also present in that section a model of a discrete–time adaptive control application having a Chenciner point on a primary Hopf curve, a secondary Hopf curve connecting two "Takens-Bogdanov" points on the boundaries of a primary resonance region, an angular degeneracy on the secondary Hopf curve, and banana–shaped secondary resonance regions.

The main areas of emphasis of the paper are determining a model, or normal form, for a Hopf bifurcation with an angular degeneracy, investigating nearby resonance surfaces and their projections to parameter space, relating this bifurcation information for the model to the bifurcation picture for a generic two-parameter family of maps with a Hopf bifurcation with an angular degeneracy, and describing situations in which the angular degeneracy is expected to occur. The main result (Theorem 2.5 and its corollary) is that the resonance regions near a generic Hopf bifurcation point with an angular degeneracy "look" either like those near point D_1 or like those near point D_2 in Figure 1b. We also discuss more global results about parameter space regions where "banana" resonance regions are expected to appear.

The paper is organized as follows. In Section 2, we recall some basic results about Hopf bifurcations, present the (known) Arnold theory for individual resonance "horns" (with emphasis on the resonance surfaces and using variations on Arnold's proofs), present analogous results for resonance regions near an angular degeneracy, and then consider the implications for the full bifurcation picture near an angular degeneracy. In Section 3, we describe scenarios in which secondary Hopf bifurcations with angular degeneracies are expected to occur, and present the adaptive control model. We discuss global parameter space "bananas" in Section 4, and make final comments in Section 5.

2. Local resonance regions near a Hopf bifurcation.

2.1. Background. We begin by recalling some standard terminology and results about Hopf bifurcations and normal forms.

Definition: A p/q resonant Hopf bifurcation point is a Hopf bifurcation point having eigenvalues $e^{\pm 2\pi ip/q}$ and rotation number of p/q around the fixed point for (an appropriate lift of) the linearization of the map at the Hopf point. The fraction p/q must be in lowest terms. If $q \geq 5$, the bifurcation is said to be **weakly resonant**; if $3 \leq q \leq 4$, it is said to be **strongly resonant**. (Sometimes $q = 1$ and $q = 2$ are called strong resonances as well, although the eigenvalues for those cases are real.)

Note that, for a fixed choice of p/q, the p/q resonant Hopf bifurcation is a codimension-two bifurcation — one parameter is needed to bring the norm of the fixed-point eigenvalue to one, and the other parameter is needed to bring the argument of the fixed-point eigenvalue to the appropriate value of $2\pi p/q$.

THEOREM 2.1 (Normal form theorem). *Let $(\mathbf{x}_0, \boldsymbol{\mu}_0)$ be a Hopf bifurcation point for the k-parameter family of functions $\mathbf{F}_\mu : \mathbf{R}^2 \to \mathbf{R}^2$, C^∞ as a function from $\mathbf{R}^2 \times \mathbf{R}^k \to \mathbf{R}^2$. Then there exists a neighborhood of $\boldsymbol{\mu}_0$ in the parameter space for which the original family can be converted by a polynomial change of variables into the form*

$$\mathbf{f}_\mu(\mathbf{z}) = e^{\rho(\mu)+i\phi(\mu)}(\mathbf{z} + A(\boldsymbol{\mu})\mathbf{z}^2\overline{\mathbf{z}} + ... + B(\mu)\overline{\mathbf{z}}^{q-1} + ...), \tag{1}$$

by identifying $\mathbf{x} \in \mathbf{R}^2$ with $\mathbf{z} \in \mathbf{C}$, a translation (to bring the unique fixed point at each parameter value to the origin), and a "near identity" polynomial change of variables. $A(\boldsymbol{\mu}) = A_1(\boldsymbol{\mu}) + iA_2(\boldsymbol{\mu})$ and $B(\boldsymbol{\mu}) = B_1(\boldsymbol{\mu}) + iB_2(\boldsymbol{\mu})$ are complex valued functions. The omitted terms are all $O(|\mathbf{z}|^{q+1})$, except possibly for those of the form $\mathbf{z}^j\overline{\mathbf{z}}^{j-1}, j \geq 3$ which are $O(|\mathbf{z}|^5)$. These "intermediate order" omitted terms are all invariant with respect to rotations; the $\overline{\mathbf{z}}^{q-1}$ term is the lowest order term in the normal form which is not invariant with respect to all rotations. The dependence of all the functions with respect to $\boldsymbol{\mu}$ is C^∞.

Proof. See any of [Ar], [GH], [Ru], for example. □

THEOREM 2.2 (Hopf bifurcation theorem). *Let $\mathbf{F}_\mu : \mathbf{R}^2 \to \mathbf{R}^2$ be a family of functions for which $\mathbf{F} : (\boldsymbol{\mu}, \mathbf{x}) \to \mathbf{F}_\mu(\mathbf{x})$ is C^∞. Assume the eigenvalue crossing condition holds at $(\mathbf{x}_0, \boldsymbol{\mu}_0)$ and that this point is not strongly resonant. Then*

1. *There is a unique fixed point near $\mathbf{x}_0$ for all maps near $\boldsymbol{\mu}_0$ in the parameter space. A C^∞-smooth "Hopf bifurcation curve", defined by the neutral linear stability of the corresponding fixed point, passes through the point $(\mathbf{x}_0, \boldsymbol{\mu}_0)$ in the parameter plane. The fixed point is stable on one side of the Hopf curve and unstable on the other side.*

2. *If in the normal form of equation (1) $A_1(\boldsymbol{\mu}_0)$ is negative (positive), then an attracting (repelling) invariant circle surrounding the fixed point is born from the fixed point as the parameter crosses the Hopf bifurcation curve from the side with the attracting fixed point to the side with the repelling fixed point (from the side with the repelling fixed point to the side with the attracting fixed point). The smoothness of the invariant circles can be guaranteed to be C^r for any $r < \infty$ by suitably restricting the parameter space neighborhood of $\boldsymbol{\mu}_0$. Local recurrent points are the fixed point and some points on the invariant circle, when the circle exists.*

Proof.

1. The existence of a unique fixed point follows from the implicit function theorem. The stability follows from the Hartman-Grobman theorem.

2. See Ruelle's textbook [Ru] for a proof of this part of the theorem using the technique of graph transforms.

□

When $A_1(\boldsymbol{\mu}_0) < 0$, the Hopf bifurcation is called **supercritical**; when $A_1(\boldsymbol{\mu}_0) > 0$, the bifurcation is called **subcritical**; when $A_1(\boldsymbol{\mu}_0) = 0$, the bifurcation is called **transcritical** or a **Chenciner** point.

2.2. Individual nondegenerate resonance surfaces and regions (à la Arnold). The Hopf bifurcation theorem implies that the bifurcation study would be complete if we knew how to divide the parameter space on the side of the Hopf curve with the invariant circle into topological equivalence classes. Consequently, we begin by studying surfaces in phase × parameter space corresponding to periodic orbits of a certain period. We first present a nondegenerate two-parameter model for investigating a "resonant" Hopf bifurcation in the neighborhood of a fixed point with eigenvalues $e^{\pm 2\pi ip/q}$. We will locate all local period-q points in a family containing such a resonant Hopf point. They will usually live on the invariant circle guaranteed by the Hopf bifurcation theorem. Although the results in this subsection are not new (cf. Arnold [Ar]), we include the subsection for several reasons: to emphasize the surfaces in phase × parameter space instead of just their projection to parameter space, to highlight the differences between the nondegenerate and the degenerate cases, to present some proofs which are slightly different from Arnold's proofs, and to make the paper more self-contained.

Arnold's analysis begins by studying vector fields which are invariant with respect to rotations of $e^{2\pi ip/q}$. He then shows that the q^{th} iterates of maps such as the model families in (2) and (3) below are, up to arbitrarily high order, "time-one" maps of these "equivariant" vector fields. In contrast, we have chosen to work directly with maps, and for $q \geq 5$, although many of our arguments are suggested by his analysis, especially for his $q = 4$ case.

Our model family of maps near a p/q resonant Hopf bifurcation point is:

$$\mathbf{f}_{(\rho,\alpha)}(\mathbf{z}) = e^{2\pi ip/q} e^{\rho + i\alpha}(\mathbf{z} + A\mathbf{z}^2\overline{\mathbf{z}} + B\overline{\mathbf{z}}^{q-1}) \tag{2}$$

where ρ and α are small real parameters, $\mathbf{z}$ is a complex variable, $\overline{\mathbf{z}}$ is its complex conjugate, p and q are integers, and $A = A_1 + iA_2$ and $B = B_1 + iB_2$ are complex constants with $A_1 \neq 0, B \neq 0$. We consider only the local bifurcation for $\mathbf{z}, \rho, \alpha$ near $\mathbf{0}, 0$, and 0, respectively. Our justification for using this model is in the proof of Corollary 2.4 below, where we show that a generic family near a p/q resonant Hopf point can be changed into the form of equation (2) plus some "higher order" terms.

Properties of the (Nondegenerate) Resonant Hopf Model. For the family defined by equation (2), which satisfies the hypotheses of the Hopf bifurcation theorem if $q \geq 5$, the fixed point $z = \mathbf{0}$ has eigenvalue $e^{\rho + i(\alpha + 2\pi p/q)}$. (The corresponding fixed point for the map in $\mathbf{R}^2$, obtained by identifying $\mathbf{R}^2$ with $\mathbf{C}$, has eigenvalues $e^{\rho \pm i(\alpha + 2\pi p/q)}$.) The line $\rho = 0$, where the origin $\mathbf{z} = 0$ changes from attracting ($\rho < 0$) to repelling ($\rho > 0$), is a Hopf bifurcation curve. The argument of the eigenvalue is monotonic along the Hopf curve. In fact, it equals $\alpha + 2\pi p/q$ at $(\rho, \alpha) = (0, \alpha)$. (Contrast this with the degenerate model, where this monotonicity fails to hold, in the next subsection.)

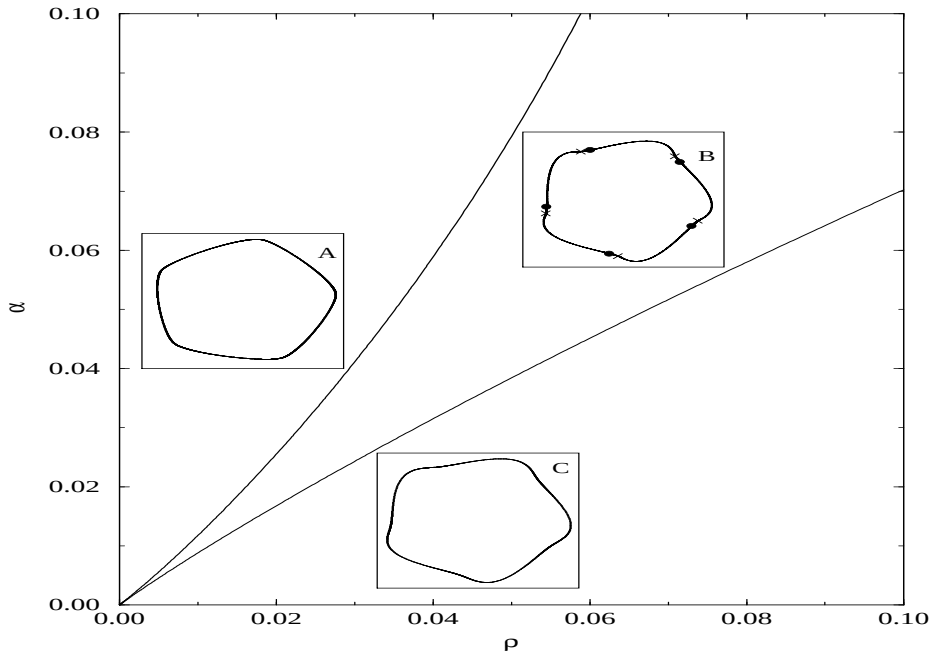

FIG. 2. *The nondegenerate Hopf model.*

The local p/q resonance region, where period-q orbits exist, for equation (2), with $p/q = 1/5, A = -1 - i, B = 1$, is the horn-shaped region in Figure 2. All three representative phase portraits are for the 5th iterate of the map. In phase portrait A, the 5th iterates rotate counterclockwise on the (attracting) invariant circle; in C they rotate clockwise; in B they move from saddles ($\times$'s) toward nodes (filled circles).

More formally, we restate the following (known) theorem.

THEOREM 2.3. *Assume the family* $\mathbf{f}_{(\rho,\alpha)}$ *is defined as in (2) and* $q \geq 5$. *Then there exists a closed neighborhood N of the origin in the phase* $\times$ *parameter space with the following properties:*

1. *The set of least-period-q (p/q) points in N is topologically a punctured (closed) disk. The puncture point is the origin – the p/q resonant Hopf bifurcation point which is a fixed point. The union of the least-period-q points and the fixed point is a closed disk.*

2. *If* $A_1 \neq 0$, *then the projection of the least-period-q (p/q) points in N to the parameter space is an (Arnold) resonance horn, emanating from the origin in the parameter space, with both sides tangent to the vector* $(-A_1, -A_2)$. *If, in addition,* $B \neq 0$, *the horns have positive measure, and the order of tangency is* $\frac{q-2}{2}$. *The parameter values near* $(\rho, \alpha) = (0, 0)$ *for which the corresponding maps have period-q orbit(s) near* $\mathbf{z} = \mathbf{0}$ *are precisely those inside and on the boundary of the resonance horn, excluding the tip of the horn, to which the p/q resonant Hopf point projects.*

3. *In the interior of this horn, there exists a pair of period-q (p/q) orbits, one attracting and one repelling when restricted to the invariant circle. The two orbits meet in a single saddle-node orbit on the boundaries of the horn (excluding the resonant Hopf point itself).*

Proof.

1. We determine all period-q points by looking at all solutions to $\mathbf{f}^q(\mathbf{z}) - \mathbf{z} = \mathbf{0}$

which are not fixed points. Expanding in terms of the parameters ρ and α and the modulus of $\mathbf{z}$, solving for the parameters, and neglecting higher order terms leads to the result.

2. Eliminate the phase variables from the expressions obtained for the proof of the above item.

3. Follow arguments similar to those of Arnold [Ar].

Details are in the Appendix. □

COROLLARY 2.4. *: Let $\mathbf{F}_\mu : \mathbf{R}^2 \to \mathbf{R}^2$ be a family of maps which satisfies the hypotheses of the Hopf bifurcation theorem as stated in Section 2.1. Assume also that $(\mathbf{x}_0, \boldsymbol{\mu}_0)$ is a p/q weakly resonant Hopf bifurcation point (defined also in Section 2.1), without a parametric degeneracy (defined in the introduction). Then there is a neighborhood of $(\mathbf{x}_0, \boldsymbol{\mu}_0)$ in the phase $\times$ parameter space in which the conclusions of Theorem 2.3 will hold, where in item 2, A is replaced by $A(\boldsymbol{\mu}_0)$, B is replaced by $B(\boldsymbol{\mu}_0)$, and the vector to which the resonance horn is tangent, is the vector that $-A(\boldsymbol{\mu}_0)$ is mapped to by the linearization of the coordinate change from the (ρ, α) parameter space to the original μ parameter space.*

Proof. Change variables to bring the original equation into the form of equation (2) plus some higher order terms. Details are in the Appendix. □

2.3. Resonance surfaces and regions near an angular degeneracy. Our model family of maps having least-period-q points near an angular degeneracy is:

$$\mathbf{f}_{(\rho,\tau)}(\mathbf{z}) = e^{2\pi i\omega_0} e^{\rho + i(c_1\rho + c_2\tau^2)}(\mathbf{z} + A\mathbf{z}^2\overline{\mathbf{z}} + B\overline{\mathbf{z}}^{q-1}) \tag{3}$$

where ρ and τ are real parameters, $\mathbf{z}$ is a complex variable, $\overline{\mathbf{z}}$ is its complex conjugate, q is an integer, ω_0 is a real constant, c_1 and $c_2 \neq 0$ are real constants, and $A = A_1 + iA_2$ and $B = B_1 + iB_2$ are complex constants. As before, we consider only the local bifurcation for $\mathbf{z}, \rho, \tau$ near $\mathbf{0}, 0$, and 0, respectively. The use of this model is justified in 2.6.

As with the nondegenerate family in (2), this family has a Hopf bifurcation along $\rho = 0$. This family is "degenerate" because the argument of the fixed-point eigenvalue, $2\pi\omega_0 + c_1\rho + c_2\tau^2$, does not vary monotonically along the Hopf curve $\rho = 0$ as τ passes through zero. This causes a change in the appearance of the resonance regions, as we now describe in 2.5.

THEOREM 2.5. [Properties of the Degenerate Hopf Model]*: Assume the family $\mathbf{f}_{(\rho,\tau)}$ is defined as in (3) and $q \geq 5$. Assume A_1, c_2, and $A_2 - c_1A_1$ are all nonzero, and $\omega_0 \neq p/q$, but is sufficiently close to p/q. Then, there is a closed neighborhood N of the origin in the phase $\times$ parameter space with the following properties:*

1. *The set of least-period-q (p/q) points in N and the projection of this set to the parameter space is described by one of four cases. If we define $\alpha_0 := 2\pi(\omega_0 - p/q)$, then the four cases are determined by the signs of the three quantities A_1, $\frac{A_2 - c_1A_1}{c_2A_1}$, and $\frac{\alpha_0 A_1}{A_2 - c_1A_1}$, as indicated respectively in the following list:*

a. (−,−,+) or (+,+,−): A twice-punctured sphere which projects to a "banana-shaped" region with both tips on the Hopf line.

b. (+,−,+) or (−,+,−): Two disjoint punctured closed disks, each projecting to disjoint resonance horns, each with its tip on the Hopf line (a "banana split").

c. (−,+,+) or (+,−,−): A closed cylinder which projects to a "thickened" parabolic region.

d. (−,−,−) or (+,+,+): The empty set (projecting to the empty set).

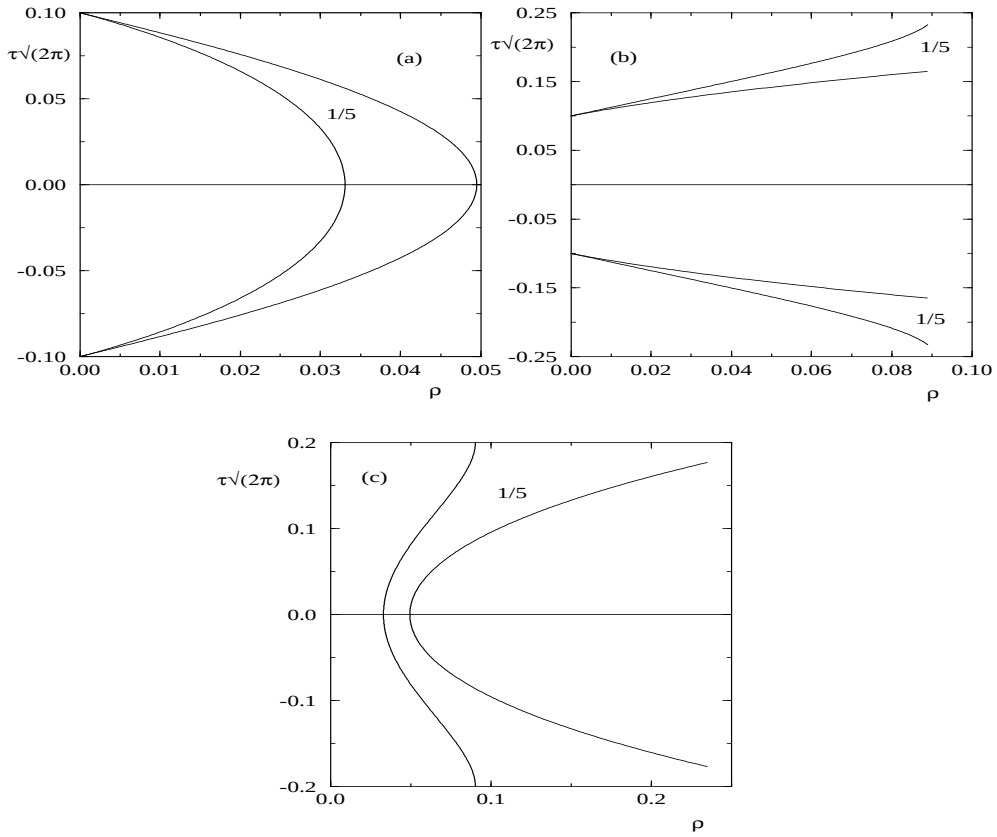

FIG. 3. *Period-5 resonance regions near a Hopf point with an angular degeneracy. Computations were done using equation (3) with* $A = -1 - i, B = 1, c_1 = -0.5$, *and (a)* $\omega_0 = 0.21, c_2 = -1$ *(b)* $\omega_0 = 0.19, c_2 = +1$ *(c)* $\omega_0 = 0.21, c_2 = +1$

The punctures, present in the first two cases, are p/q resonant Hopf points located at $(\mathbf{z}, (\rho, \tau)) = (\mathbf{0}, (0, \pm\sqrt{-\alpha_0/c_2}))$, *and project to corresponding horn tips. If* $B \neq 0$, *the parameter space horns have positive measure and have order of tangency* $\frac{q-2}{2}$ *at the tips. In all cases, the "centers" of the horns are pieces of parabolas to lowest order. The parameter values near* $(\rho, \tau) = (0, 0)$, *for which the corresponding maps have least-period-q (p/q) orbit(s) near* $\mathbf{z} = \mathbf{0}$, *are precisely those inside and on the boundary of the resonance region(s), excluding the resonant fixed points which project to the horn tips.*

1. *On the interior of this region(s), there exists a pair of period-q (p/q) orbits, one attracting and one repelling, when restricted to the invariant circle. The two orbits meet in a single saddle-node orbit on the boundaries of the horn (excluding the resonant Hopf point(s) itself).*

Note: The terms in quotations are made more precise in the proof. Parameter space projections of cases (a), (b), and (c) are illustrated in Figures 3a, 3b, 3c, respectively.

Proof.

1. The nondegenerate family of equation (2) and the degenerate family of equation (3) differ only in the appearance of their parameters: α has now been replaced by $\alpha_0 + c_1\rho + c_2\tau^2$. The proof is thus obtained by a (noninjective) change of parameters.

Details are in the Appendix. See also the end of the next subsection, where with the aid of Figure 4 we describe geometrically how the degenerate parameter space "unfolds" onto the nondegenerate parameter space.

2. Same as the proof of item 3 in Theorem 2.3.

□

For the statement of the following corollary, we recall notation from the introduction: $\mu(s)$ is an arclength parametrization of the Hopf curve which passes through the bifurcation point at $s = 0$, and $e^{\rho(\mu)\pm i(2\pi\omega_o+\alpha(\mu))}$ are the eigenvalues of the corresponding fixed point along the Hopf curve.

COROLLARY 2.6. *Let $\mathbf{F}_\mu : \mathbf{R}^2 \to \mathbf{R}^2$ be a family of maps which satisfies the hypotheses of the Hopf bifurcation theorem as stated in Section 2.1, including the eigenvalue crossing condition. Assume that $(\mathbf{x}_0, \boldsymbol{\mu}_0)$ is a Hopf bifurcation point with an angular degeneracy (defined in the introduction), the eigenvalues of $D\mathbf{F}_{\mu_0}(\mathbf{x}_0)$ are $e^{\pm 2\pi i\omega_0}$, the rotation number around $\mathbf{x}_0$ of (a lift of) $D\mathbf{F}_{\mu_0}(\mathbf{x}_0)$ is $+\omega_0$, and $\omega_0 \neq p/q$ for $q \leq 4$ (not strongly resonant).*

Assume also that and $\nabla_\mu\alpha(\boldsymbol{\mu}_0) \neq \mathbf{0}$. Thus $\nabla_\mu\rho(\boldsymbol{\mu}_0)$ and $\nabla_\mu\alpha(\boldsymbol{\mu}_0)$ are nonzero parallel vectors and $\frac{d}{ds}\alpha(\boldsymbol{\mu}(s)) = 0$. Assume, however, that $\frac{d^2}{ds^2}\alpha(\boldsymbol{\mu}(s)) \neq 0$. Then for any p/q sufficiently close to ω_0, there is a closed neighborhood N of $(\mathbf{x}_0, \boldsymbol{\mu}_0)$ in the phase $\times$ parameter space inside which the set of period-q (p/q) points in N is described by one of the four cases (a) - (d) enumerated in statement 1 of Theorem 2.5. The four cases are determined in the same way as in Theorem 2.5, after putting the original equation in its normal form up to $O(|z|^3)$ terms, changing parameters from $\boldsymbol{\mu}$ to (ρ, τ), letting $A = A(\boldsymbol{\mu}_0)$, and writing the eigenvalue argument $\phi(\rho, \tau) = \omega_0 + c_1\rho + c_2\tau^2 + \ldots$, a form justified in the proof.

Proof. This proof is similar to that of Corollary 2.4. We show that there is a nonsingular change of coordinates which brings our original equation into the same form as our model with an angular degeneracy except for higher order terms. Details are in the Appendix. □

2.4. Discussion. Although the theorems and their corollaries in the previous subsection stated results for only one p/q resonance surface at a time, there are some relationships between nearby resonance surfaces we wish to point out.

First, for a p/q resonance horn away from an angular degeneracy, we recall from Corollary 2.4 that the angle at which it meets the Hopf curve is determined by the coefficient $A(\boldsymbol{\mu})$ of the $z^2\overline{z}$ term in the normal form, where $\boldsymbol{\mu}$ is the parameter value corresponding to a p/q resonant Hopf point. Since this coefficient varies smoothly along the Hopf curve, the angles at which the various resonance horns meet the Hopf curve will also vary smoothly along the Hopf curve. (No similar statement can be made about the "$B(\mu)$" coefficient of the $\overline{z}^{q-1}$ term; it is not even the coefficient of the same term in the normal form as we move from one resonant Hopf point to another). This implies that along the Hopf curve for any family, the angle at which a p/q resonance horn meets the Hopf curve varies smoothly as p/q varies. This is even true if the B coefficient in the normal form near a particular p/q resonant Hopf point is zero; the order of tangency of the saddle-node curves for that particular p/q resonance horn, however, would not be of order $\frac{q-2}{2}$.

A similar statement holds for the consistency in the shape of resonance regions near an angular degeneracy. The "parabolas" which define the "centers" of the p/q resonance regions (defined in the proof of Theorem 2.3), vary smoothly in p/q.

We also point out that, even though there are four distinct cases for individual resonance regions, the collection of resonance surfaces and regions near a single Hopf

bifurcation with an angular degeneracy has one of the following two forms:

a. Twice punctured disks which project to "bananas" for all p/q on one side of ω_0; the empty set for all p/q on the other side of ω_0.

b. Pairs of punctured disks which project to "banana splits" for all p/q on one side of ω_0; closed cylinders which project to thickened parabolas for all p/q on the other side of ω_0.

Analytically, this is because the signs of the three quantities: A_1, $\frac{A_2 - c_1 A_1}{c_2 A_1}$, and $\frac{\alpha_0 A_1}{A_2 - c_1 A_1}$, determine the four cases; only the last quantity can change sign as p/q is varied (via $\alpha_0 := 2\pi(\omega_0 - p/q)$).

The first case is illustrated schematically in Figure 1b near point D_1 and for the model family below in Figure $4d_1$. The second case is illustrated schematically in Figure 1b near point D_2 and for the model family below in Figure $4d_2$. See also Figure 10, described in the proof of Theorem 2.5 in the Appendix, for a further description of how nearby resonance regions change as varying p/q causes α_0 to change between positive and negative.

MODEL FAMILY. To portray a bifurcation picture with more than one resonance region near an angular degeneracy, we used the following family:

$$\mathbf{f}_{(\rho,\tau)}(\mathbf{z}) = e^{2\pi i \omega_0} e^{\rho + i(c_1\rho + c_2\tau^2)}(\mathbf{z} + A\mathbf{z}^2\overline{\mathbf{z}} + B\overline{\mathbf{z}}^{q-1} + C\mathbf{z}^3\overline{\mathbf{z}}) \tag{4}$$

with $\omega_0 = 0.19, c_1 = -0.5, A = -1 - i, B = 1, C = 1, q = 5$. Figure $4d_1$, using $c_2 = -1$, shows two banana resonance regions; Figure $4d_2$, using $c_2 = +1$, shows a banana split resonance region and two parabolic resonance regions.

The family of equation (4) is the same as the model degenerate family we began with in Equation (3), except for the $\mathbf{z}^3\overline{\mathbf{z}}$ term. We made this alteration because the family of equation (3) is invariant to rotations by $2\pi p/q$. This is fine for computing the p/q resonance region, but not for any other resonance region. For example, if $p/q = 1/5$, and we were computing the $1/6$ resonance region, the invariance with respect to rotations by $2\pi/5$ would imply that period-6 orbits must appear in groups of 5. Thus, a saddle-node birth of a pair of period-6 orbits would result in the birth of 10 period-6 orbits, or 60 period-6 points. The $\mathbf{z}^3\overline{\mathbf{z}}$ term was chosen because it is of high enough order so as not to affect the existence of the invariant circle, and because it is not invariant to any rotations about the origin in phase space. Thus no unwanted symmetries are present.

The Geometry of the parameter change or, "Theorem 2.3 to Theorem 2.5 in pictures". Figures $4d_1$ and $4d_2$ can be thought of as having been created via parameter space "surgeries" of a bifurcation diagram for a corresponding nondegenerate family. Specifically, if we start with the bifurcation diagram of Figure $4a$ for the nondegenerate family $\mathbf{f}_{(\rho,\alpha)}(\mathbf{z}) = e^{\rho + i\alpha}(\mathbf{z} + A\mathbf{z}^2\overline{\mathbf{z}} + B\overline{\mathbf{z}}^{q-1} + C\mathbf{z}^3\overline{\mathbf{z}})$, we can change it into either Figure $4\mathrm{d}_1$ or $4\mathrm{d}_2$ with the coordinate change $\alpha = 2\pi\omega_0 + c_1\rho + c_2\tau^2$. This coordinate change, replacing α with τ, can be decomposed into the following three coordinate changes, each having a simple geometric interpretation:

a. A shear to make the "singular line" perpendicular to the Hopf curve: $\alpha = \hat{\alpha} + c_1\rho$. (Figure 4a to 4b.)

b. "Unfolding a double cover of half of the nondegenerate parameter space:" $\hat{\alpha} = 2\pi\omega_0 + c_2|\hat{\tau}|, c_2 = \pm 1$. (Figure 4b to $4c_1$ for $c_2 = 1$; Figure 4b to $4c_2$ for $c_2 = -1$.)

c. Smooth at the fold lines: $\hat{\tau} = \tau|\tau|$. (Figure $4\mathrm{c}_1$ to $4d_1$ or Figure $4\mathrm{c}_2$ to $4d_2$.)

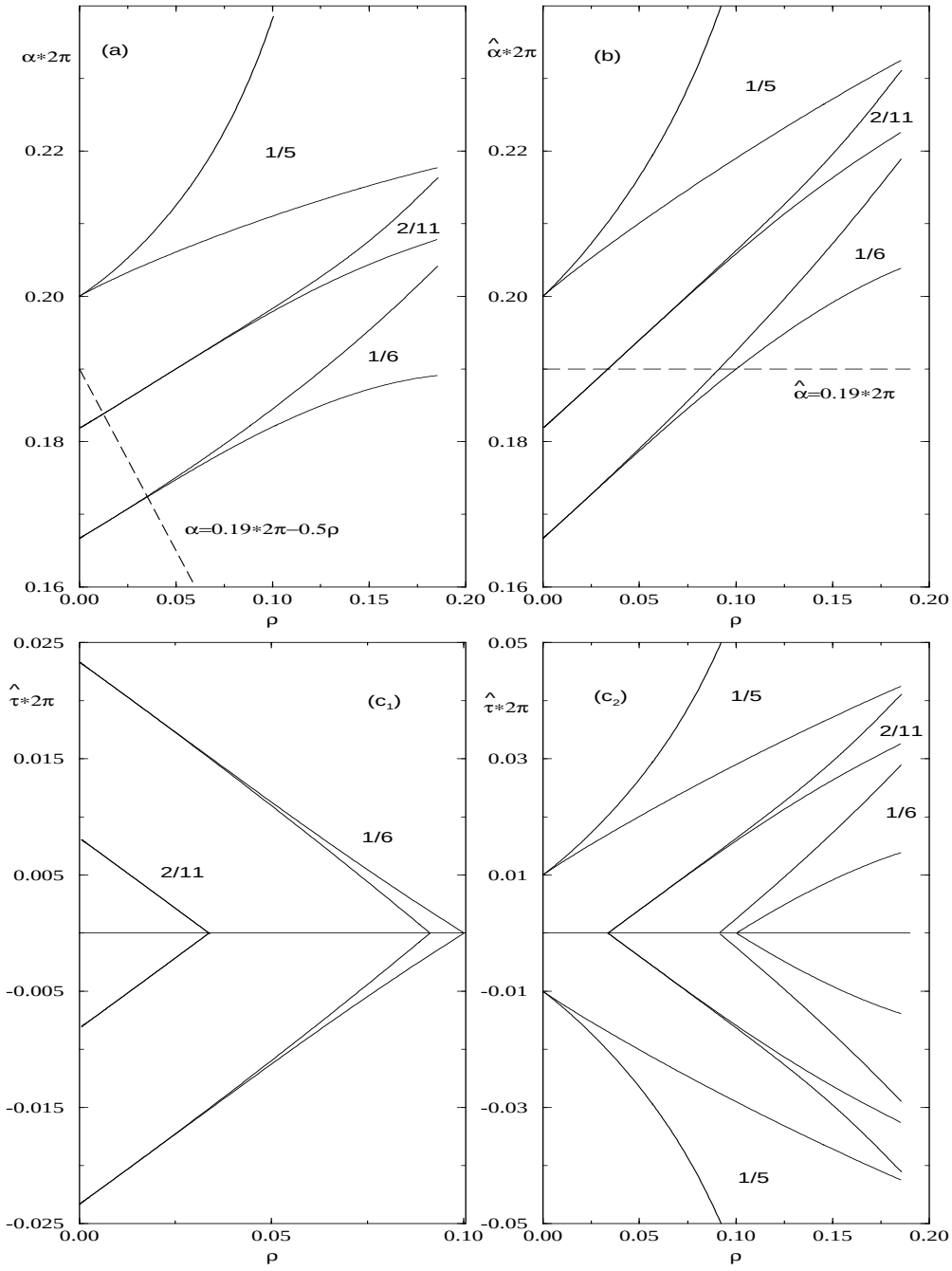

A rescaling would give the same picture as Figure 4d$_1$ for any negative c_2, and the same picture as Figure 4d$_2$ for any positive c_2.

It is now easier to see why the nondegeneracy conditions of Theorem 2.5 are necessary. The value of A_1 must be nonzero so that the resonance horns emerge transverse to the Hopf curve. The expression $A_2 - c_1 A_1$ must be nonzero to ensure the resonance horns cross the fold line transversely (the horns emerge with slope $\frac{A_2}{A_1}$ and the slope of the fold line is c_1). If c_2 were zero, the fold might be even more

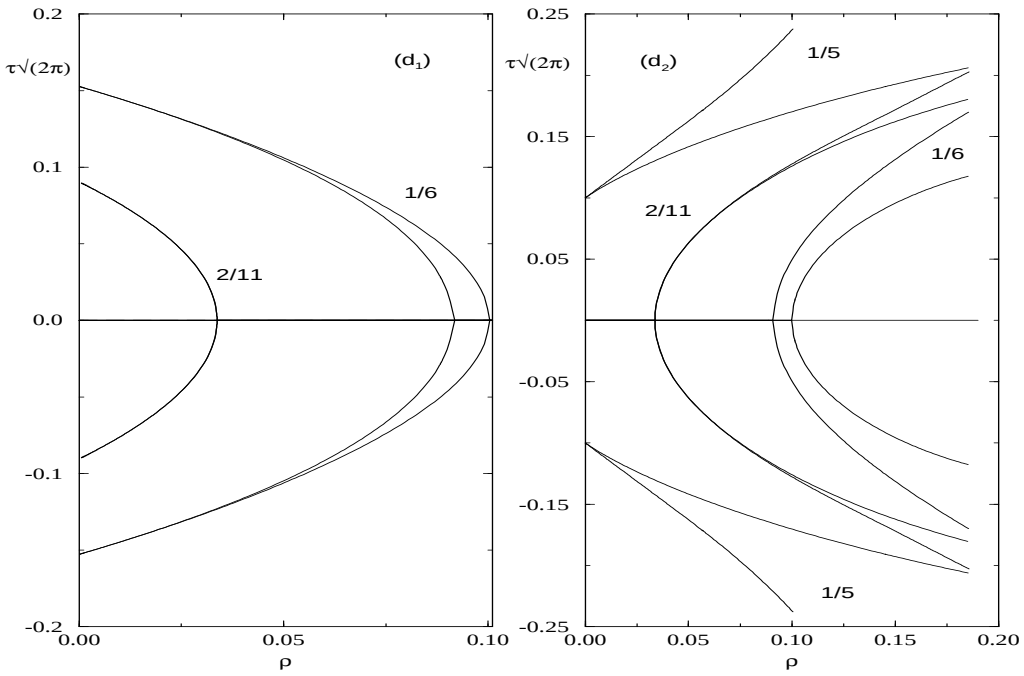

FIG. 4. *Relationship of the nondegenerate parameter space to the degenerate one: (a)* $\mathbf{f}_{(\rho,\alpha)}(\mathbf{z}) = e^{2\pi i\omega_0}e^{\rho+i\alpha}(\mathbf{z} + A\mathbf{z}^2\overline{\mathbf{z}} + B\overline{\mathbf{z}}^{q-1} + C\mathbf{z}^3\overline{\mathbf{z}})$*; (b)* $\mathbf{f}_{(\rho,\dot{\alpha})}(\mathbf{z}) = e^{2\pi i\omega_0}e^{\rho+i(\dot{\alpha}+c_1\rho)}(\mathbf{z} + A\mathbf{z}^2\overline{\mathbf{z}} + B\overline{\mathbf{z}}^{q-1} + C\mathbf{z}^3\overline{\mathbf{z}})$*; (c)* $\mathbf{f}_{(\rho,\dot{\tau})}(\mathbf{z}) = e^{2\pi i\omega_0}e^{\rho+i(2\pi\omega_0+c_1\rho+c_2|\dot{\tau}|)}(\mathbf{z} + A\mathbf{z}^2\overline{\mathbf{z}} + B\overline{\mathbf{z}}^{q-1} + C\mathbf{z}^3\overline{\mathbf{z}})$*; (d)* $\mathbf{f}_{(\rho,\tau)}(\mathbf{z}) = e^{2\pi i\omega_0}e^{\rho+i(c_1\rho+c_2\tau^2)}(\mathbf{z}+A\mathbf{z}^2\overline{\mathbf{z}}+B\overline{\mathbf{z}}^{q-1}+C\mathbf{z}^3\overline{\mathbf{z}})$ *In all figures,* $\omega_0 = 0.19, c_1 = -0.5, A = -1-i, B = 1, C = 1, q = 5$*; in* c_1 *and* d_1*, the constant* $c_2 = -1$*; in* c_2 *and* d_2*, the constant* $c_2 = +1$.

degenerate.

More general degenerate families could also be considered as geometric unfoldings of a double cover of half a nondegenerate parameter space, but only to lowest order terms. The model families behave better because they have constant coefficients A and B; in a more general family these coefficients would depend on the parameters.

3. Angular Degeneracies on Secondary Hopf bifurcation curves. So far, the only reason we have given for expecting a Hopf bifurcation with an angular degeneracy is that the relationship between an application's natural parameters and the "universal" parameters, the modulus and argument of a fixed point's eigenvalue, could be nonhomeomorphic. We now describe some scenarios in which the angular degeneracy is expected, or even guaranteed, to occur, even for the "best" choice of parametrizations. They all involve secondary, rather than primary, Hopf bifurcations. These scenarios, in fact, were the original motivation behind our study of a Hopf bifurcation with an angular degeneracy which led to this paper.

3.1. Takens–Bogdanov points and secondary bifurcations. When a fixed point of a family $\mathbf{F}_\mu$ undergoes a (primary) Hopf bifurcation, one result can be the birth of periodic orbits as the Hopf curve in the parameter plane is crossed. Period-q resonance regions (horns), described throughout this paper, where period-q orbits exist, emanate from a point on the primary Hopf curve where the eigenvalues of $D\mathbf{F}_\mu$ at the associated fixed point are located at a q^{th} root of unity.

The sides of a period-q resonance region are period-q saddle-node bifurcation curves, characterized by having an eigenvalue of $D\mathbf{F}_\mu^q$ at one. As a saddle-node curve is traced out in the parameter space, away from the primary Hopf bifurcation, the second eigenvalue may vary. (For $q \geq 5$ and parameter values near the primary Hopf bifurcation, the second eigenvalue determines the local attraction or repulsion normal to the invariant curve.) If the second eigenvalue also becomes equal to one, we generically have a double 1, or "Takens-Bogdanov" point [Bo,Ta]. One consequence of the analysis of a generic Takens-Bogdanov point is the emergence of a (secondary) Hopf curve from the Takens-Bogdanov point, tangent to the saddle-node and extending *into* the primary resonance region. This secondary Hopf curve is characterized by the existence of a period-q point where the eigenvalues of $D\mathbf{F}_\mu^q$ are complex conjugate and on the unit circle. A (secondary) period-mq resonance horn, analogous to a primary period-m resonance horn, will emanate from a point on the secondary Hopf curve where $D\mathbf{F}_\mu^q$ at the associated period-q point has an eigenvalue at an m^{th} root of unity.

Only five possibilities exist for the global continuation of a Hopf curve in a two-parameter family: (1) continuation in each direction terminates at a Takens-Bogdanov point, (2) continuation in each direction terminates at a "double -1 point" [Ar, Ta], (3) continuation in one direction terminates at a Takens-Bogdanov point, continuation in the other direction terminates at a double -1 point, (4) continuation forms a closed curve, or (5) continuation proceeds forever (in an unbounded parameter space). Possibilities (1) and (2) imply the existence of local extrema for the argument of the neutral eigenvalue along the Hopf curve. These local extrema are generically the Hopf bifurcation points with angular degeneracies.

Several possible scenarios, all involving secondary Hopf bifurcations and most involving Takens-Bogdanov points, are suggested in Figures 5a–e. In Figures 5a–d, we can assume the eigenvalue argument is zero at one of the Takens-Bogdanov points. Continuity of this eigenvalue along the secondary Hopf bifurcation curve, coupled with the assumed fact that no double -1 points are encountered along the way, implies that the argument must return to zero at the other Takens–Bogdanov point. Thus the argument (generically non-constant) must reach a maximum or minimum at least once along the secondary Hopf curve. In Figure 5e, if by moving all the way around the secondary Hopf curve also returns the secondary rotation number to its value at the starting point, then relative extrema must exist. Thus, these scenarios will lead to Hopf bifurcations with angular degeneracies.

Differences in the figures depend on which side of the horn the second Takens-Bogdanov point appears, which side of the secondary Hopf bifurcation curve the secondary invariant curves exist, and on which type of angular degeneracy is realized ("banana" vs. "banana split"). Although there are no Takens-Bogdanov points in Figure 5e, it could turn into Figure 5d by "expanding" the secondary Hopf circle through a variation of an auxiliary parameter, for example, until the "top" angular degeneracy "hit" the saddle-node curves bounding the resonance horn. Other similar scenarios are also possible.

Figure 5a is an illustration of a pair of resonance horns which exist near a "Chenciner" point [Ch] . A Chenciner point is yet another degenerate Hopf bifurcation point: the Hopf bifurcations change between supercritical and subcritical at the Chenciner point. This is illustrated by the switch in the side of the primary Hopf bifurcation curve to which the primary resonance horns grow. As part of his thesis, Johnson [Jo] showed that there *necessarily* exist two Takens-Bogdanov points, one on

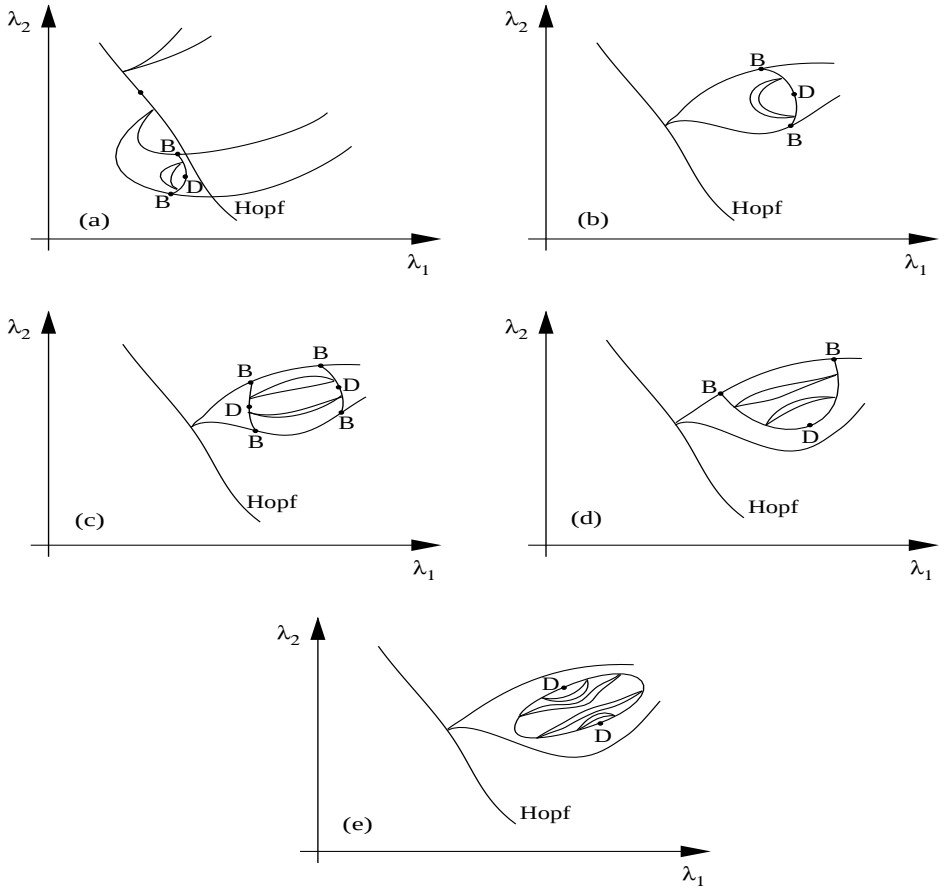

FIG. 5. *Angular degeneracies D due to Bogdanov points B.*

each side of the primary resonance horn which "turns around", and a secondary Hopf curve which connects them. In this case, there *must* be a Hopf point with an angular degeneracy along that secondary Hopf bifurcation curve. The adaptive control application, which we describe next, has a bifurcation diagram with features similar to Figure 5a.

3.2. The adaptive control application. Consider the problem of controlling the linear, discrete-time, single-input, single-output (SISO), plant with unknown, constant coefficients (see the 1984 textbook by Goodwin & Sin [GS]):

$$y(t+1) = -\alpha_1 y(t) - \alpha_2 y(t-1) + \beta_0 u(t). \tag{5}$$

In designing the controller, a first-order model of (5) is assumed:

$$\hat{y}(t+1) = \hat{\alpha}_1(t) y(t) + \hat{\beta} u(t) \tag{6}$$

where $-\hat{\alpha}_1$ and $\hat{\beta}$ are estimates of the actual system parameters α and β. Thus, two sources of plant/reference-model error are introduced by the reference model: (1) the use of a first-order model (since $\hat{\alpha}_2 = 0, \alpha_2$ becomes a measure of the plant/reference-model *order* mismatch); (2) it is assumed that a good estimate of the gain of the manipulated variable (β_0) is known (thus, $\hat{\beta}$ is a constant). The objective of the

controller $u(t)$ is to make the system follow the set point $y^*(t)$; inverting (6), the control law

$$u(t) = \frac{y^*(t+1) - \hat{\alpha}_1(t)y(t)}{\hat{\beta}}$$

is obtained. Choosing $y^*(t+1) = \text{constant} \neq 0$, it is possible to set $y^* = 1$ without loss of generality. The recursive identifier for α_1 is a scalar form of the projection algorithm of Goodwin *et al.*, 1980 [GRC]:

$$\hat{\alpha}_1(t) = \hat{\alpha}_1(t-1) + y(t-1)\frac{y(t)-1}{c + y(t-1)^2}.$$

Defining $x(t+1) = y(t)$, the closed-loop system can be written as

$$\begin{aligned} x(t+1) &= y(t), \\ y(t+1) &= -\alpha_1 y(t) - \alpha_2 x(t) + \frac{\beta_0}{\hat{\beta}}\left(1 - \hat{\alpha}_1(t)y(t)\right), \\ \hat{\alpha}_1(t+1) &= \hat{\alpha}_1(t) + \frac{y(t)}{c + y^2(t)}(y(t+1) - 1), \end{aligned}$$

and after defining $a = -\alpha_1$, $b = -\alpha_2$, $k = \beta_0/\hat{\beta}$, and $z = a - k\hat{\alpha}_1$ the final form of the map: G: $R^3 \mapsto R^3$

$$\begin{pmatrix} x \\ y \\ z \end{pmatrix} \mapsto \begin{pmatrix} y \\ bx + k + zy \\ z - \frac{ky}{c+y^2}(bx + k + zy - 1) \end{pmatrix}$$

is derived. The system is characterized by three parameters. The small and positive constant c pertains to the estimation algorithm chosen; it is used to prevent division by zero in the estimator. In our calculations it was kept fixed at the representative value of $c = 0.1$. The second parameter, k, is a measure of the error in the assumption of the value of the gain of the manipulated variable ($k = 1$ implies no error); and finally b is a measure of the plant/reference-model-order mismatch ($b = 0$ implies no order error).

Bifurcation analysis reveals a Hopf bifurcation locus for the period-1 fixed point (it corresponds to the set point of the process) in the (k, b) parameter plane:

$$b = b_h = -\frac{c+1}{c+2}$$

Along the Hopf-bifurcation locus, two complex eigenvalues are located on the unit circle (critical eigenvalues) while the third, real eigenvalue is given by:

$$\lambda_1 = -b_h = \frac{c+1}{c+2}.$$

Since λ_1 lies well within the unit circle for our choice of $c = 0.1$, the dynamics are strongly contracting in the direction corresponding to λ_1. It is therefore expected that the system will behave in a fashion similar to a map of the plane in the neighborhood of the Hopf bifurcation. It can be easily shown that as k is varied along the Hopf-bifurcation line, the critical eigenvalues start at (-1,-1) at $k = 2.092857$ and then move

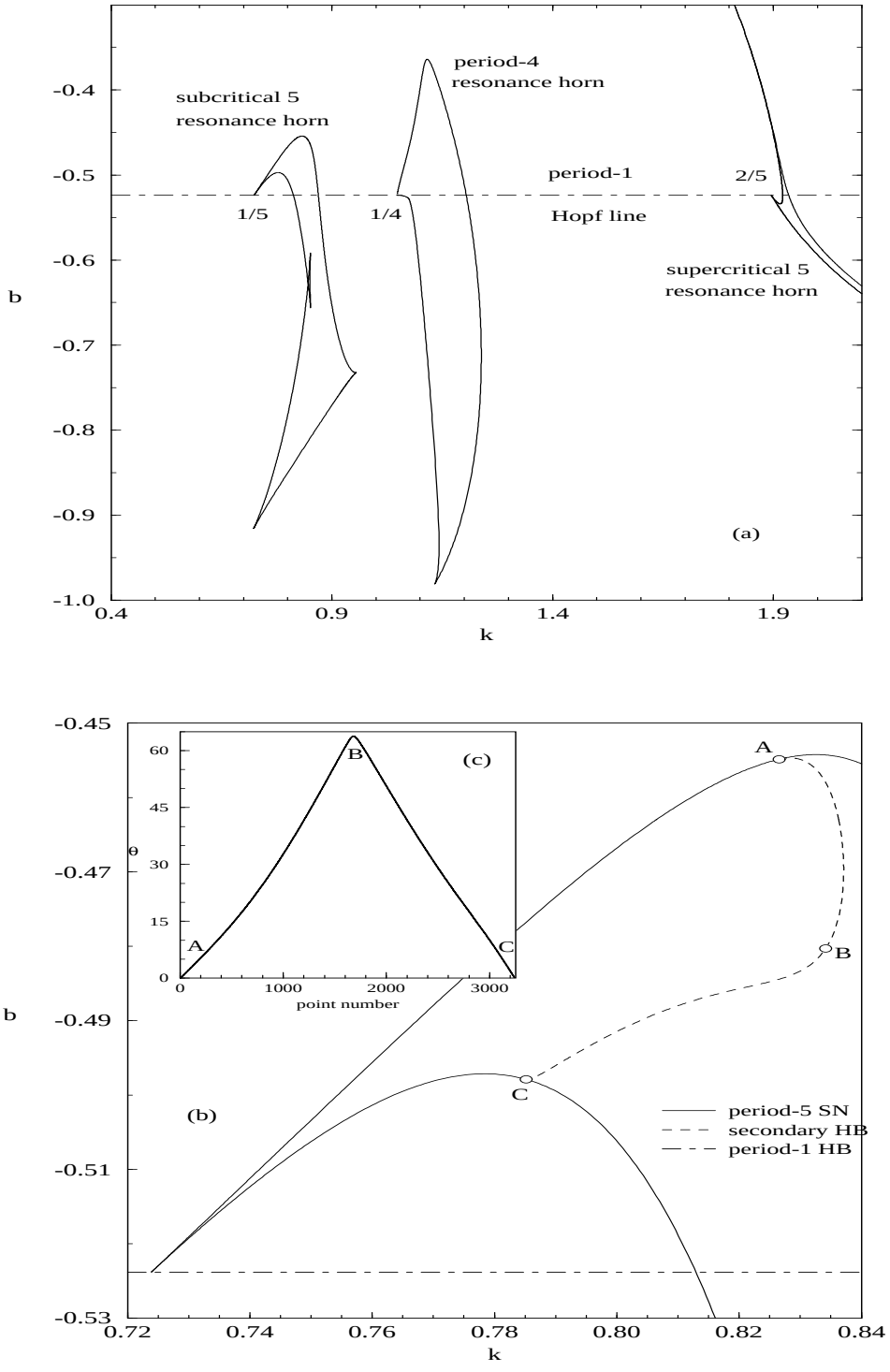

FIG. 6. *Adaptive control system: (a) Parameter Space, (b) Local bifurcations inside the subcritical period-5 horn, (c) Angle vs location on secondary Hopf curve.*

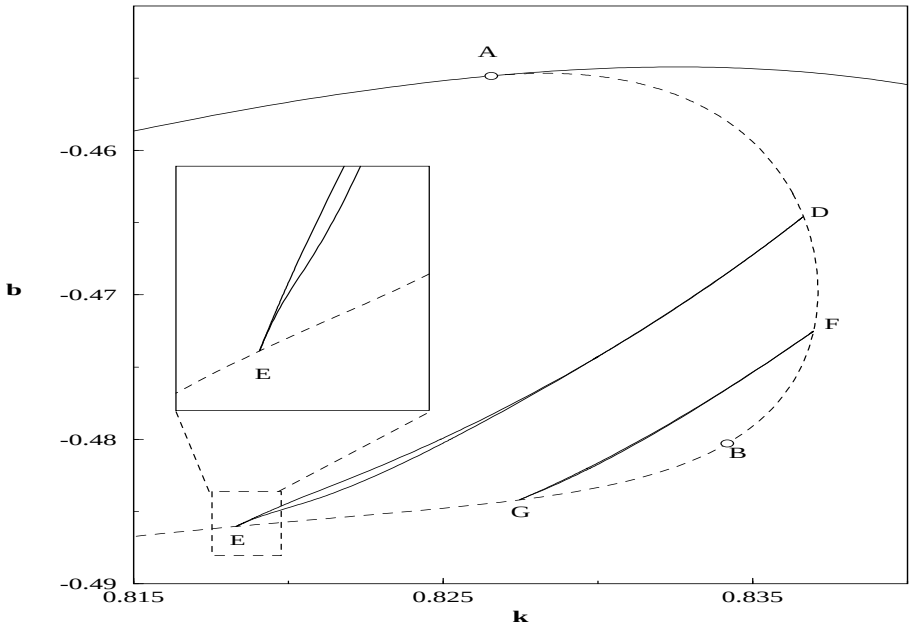

FIG. 7. *Period-30 and period-35 "bananas".*

monotonically over the entire unit circle, approaching (1,1) as $k \to 0$. As described, for example, in Corollary 2.4, primary resonance horns are expected to emanate from this line. This is confirmed in Figure 6a; the details of the local bifurcations at the tip of the subcritical period-5 horn are shown in Figure 6b (Frouzakis *et al.*, 1991 [FAK], Frouzakis, 1992 [Fr]). The continuation calculations were performed using AUTO86 by E. Doedel [Do, DK] (and a real-time graphics interface for it by Dr. M. A. Taylor in our group).

On each side of this period-5 horn we observe a Takens-Bogdanov point (two eigenvalues of $D\mathbf{G}^5$ at one); they are marked A and C in Figure 6b. As predicted by the theory, we were able to compute the secondary Hopf bifurcation curve inside the period-5 horn connecting the two Takens-Bogdanov points. Along this curve, the two relevant eigenvalues of the corresponding period-5 orbit "start" with zero argument (point A) and after reaching a maximum argument of about 63.8^o on the unit circle (point B — the angular degeneracy) they move back to zero argument at point C (Figure 6c). Secondary resonance regions originate from this secondary Hopf curve. Figure 7 shows the "banana-shaped" secondary resonance horns associated with a 6^{th} and 7^{th} root of unity, when the eigenvalues are $\cos(\frac{2\pi}{6}) \pm i\sin(\frac{2\pi}{6})$ and $\cos(\frac{2\pi}{7}) \pm i\sin(\frac{2\pi}{7})$ respectively. The 6^{th} root of unity is crossed twice along the AC curve (at points F and G) where $(k, b) \approx (0.8369, -0.4725)$ and $(0.8274, -0.48418)$ respectively. Similarly, the period-7 resonance horn opens and closes at points D and E on the AC curve, where $(k, b) \approx (0.8366, -0.4645)$ and $(0.8183, -0.48603)$ respectively. We have numerically traced the boundaries of the period-6 and period-7 resonance horns for G^5 in Figure 7. (Period-6 (resp. 7) for G^5 means period $5 * 6 = 30$ (resp. $5 * 7 = 35$) for the original map G.) These secondary resonance horns both "open" and "close" on the secondary (i.e., period-5) Hopf bifurcation curve, suggesting that point B is a "banana" point rather than a "banana split" point. We would need to

compute higher order terms in the normal form on the center manifold, however, in order to be sure.

We note that in other examples with an angular degeneracy on a secondary Hopf curve the argument of the eigenvalue at the maximum point (that is, at the angular degeneracy) is only a couple degrees instead of 63.8^o, as it is here. This is why this example was good for computing bananas: period 5×6 saddle-nodes are much easier to compute than saddle-nodes of period 5×180.

4. Global bananas. All of our results to this point have been local in nature. Banana regions or banana split/parabolic regions have been shown to exist in arbitrarily small neighborhoods of a Hopf bifurcation point with an angular degeneracy. On the other hand, banana resonance regions seem to appear in our numerically computed bifurcation diagrams even relatively far from angular degeneracies. For example, the period-30 and 35 bananas of Figure 7 seem relatively far from the angular degeneracy — far enough, at least so that their shapes would not be still called parabolic. Also, in the schematic bifurcation diagrams of Figure 5, all the secondary resonance regions are closed bananas, even in the case of Figure 5c, where the two angular degeneracies are intended to be locally banana split points. It is even possible that the saddle-node curves, which bound the primary resonance regions of Figure 5, if continued beyond the point where the diagrams stop, could "end" at a second cusp on another (or the same) primary Hopf bifurcation curve. We now give the following global banana result, where the existence of one p/q resonant Hopf point implies the existence of another.

THEOREM 4.1. *Let* $\mathbf{F}$ *be a* C^∞ *function from* $\mathbf{R}^2 \times \mathbf{R}^2 \to \mathbf{R}^2$ *which represents a two-parameter family of diffeomorphisms of the plane. Assume*

1. *There is a Hopf bifurcation curve with a* p/q *resonant point,* $q \geq 3$*, which does not have an angular degeneracy.*
2. *The region of phase* $\times$ *parameter space where a* p/q *orbit exists is compact.*

Then there must exist another p/q *resonant Hopf point somewhere in that compact region of phase* $\times$ *parameter space. Both points are puncture points on the same component of least-period-*q *points (i.e., the component of the* p/q *resonance surface) in the phase* $\times$ *parameter space. (That is, the existence of one end of a banana implies a second end must also exist.)*

Proof. Theorem 2.3 tells us that the surface of period-q points near the assumed p/q resonant Hopf point is a punctured disk. The idea of the proof is to consider this surface globally in the phase $\times$ parameter space. It can be shown that the closure of the set of least-period-q points in phase $\times$ parameter space forms an orientable topological two-manifold. (In the simplest case, this manifold would be a topological sphere, but it might have some number of handles, as well). All points on this manifold are least-period-q points under the map $(\mathbf{x}, \boldsymbol{\mu}) \to (\mathbf{F}_\mu(\mathbf{x}), \boldsymbol{\mu})$, except possibly for isolated fixed points such as the p/q resonant Hopf point projecting to the (first) tip of the resonance horn (if $q \geq 5$). The proof of the existence of the second fixed point on the resonance surface emanating from the first p/q resonant Hopf point is almost the same as the proof of Theorem 2 of [P2]. That theorem proves the existence of a p/q Hopf point on a p/q surface that emanates not from a first p/q Hopf point, but from "zero forcing amplitude" in a two-parameter family of maps of the plane generated by return maps of a periodically forced planar oscillator. The p/q surface for a forced oscillator "naturally" has an invariant circle as a boundary component; the map restricted to this invariant circle is a rigid rotation by p/q. To convert our situation to that of [P2], we need to replace the first p/q Hopf point with a boundary

circle on which the map is a rotation by p/q. But this is easily done by "blowing up" the p/q resonant Hopf point (extending the phase space in polar coordinates to $r = 0$). The proof of the existence of the second p/q Hopf point then follows from [P2]. □

We next present a corollary which describes conditions under which a whole collection of secondary global banana regions will exist.

COROLLARY 4.2. *Let $\mathbf{F}_\mu$ be a generic two-parameter family of diffeomorphisms of $\mathbf{R}^2$. Assume*

1. *There is a p/q resonance surface in the phase $\times$ parameter space resulting from a (primary) p/q resonant Hopf bifurcation.*
2. *The p/q resonance surface includes two Takens–Bogdanov points for the q^{th} iterate of the map; the two Takens–Bogdanov points are connected by a secondary Hopf bifurcation curve (also along the p/q resonance surface).*
3. *Along the secondary Hopf curve the argument of the neutral eigenvalue of $D\mathbf{F}_\mu^q$ has a single local extremum, say $2\pi\omega_0$.*
4. *There is no other secondary Hopf curve on the p/q resonance surface.*
5. *All secondary periodic point surfaces emanating from the secondary Hopf curve are contained in a compact region of phase $\times$ parameter space.*

Then, for every $m/n \in (0, \omega_0)$, the period-qn surface emanating out of the m/n secondary Hopf point must connect to the period-qn resonance surface emanating from the unique m/n Hopf point on the secondary Hopf curve on the other side of the local extremum. (Thus, all resonance regions emanating from the secondary Hopf curve are globally closed bananas.)

Proof. The hypotheses of Theorem 4.1 are satisfied for each $m/n \in (0, \omega_0)$, so a second m/n Hopf point must exist. The assumptions of a single local extremum and no other secondary Hopf curves imply that there is only one "appropriate" point. This point, therefore, is where the other end of the global banana must be. □

Note: It seems that all primary resonance horns near and on one side of a Chenciner point on a Hopf bifurcation curve satisfy the hypotheses of Corollary 4.2. This would give us an infinite collection of primary resonance horns, each having its own infinite collection of global bananas.

5. Conclusions and Comments. Although the parametric degeneracy we studied in this paper was specifically along a Hopf bifurcation curve, *any* parametric degeneracy (with respect to parameters in a universal unfolding of a local bifurcation) can be thought of, in its simplest form, as merely a local "folding in half" of the degenerate parameter space, in order to map it to the universal (nondegenerate) parameter space. We could, for example, have included the strongly resonant cases in Theorems 2.3 and 2.5 and their corollaries, even though the projections of the resonance surfaces near the strongly resonant Hopf points to the (nondegenerate) parameter space are not necessarily cusps.

It might be useful to write explicit conditions in terms of the original map to determine (a) an angular degeneracy and (b) the type: banana vs. banana-split (harder, since higher order terms are required). We found it much easier to verify conditions of the theorem by numerically computing arguments of eigenvalues along the Hopf curve, as we did for the adaptive control application to produce Figure 6c, than by computing a normal form (especially when needing to use a center manifold).

We point out that the global results (Theorem 4.1 and Corollary 4.2) are very much dependent on the phase space being two-dimensional. The fixed-point theorem from [P2] quoted in the proof of Theorem C applies only in that setting. On the other

hand, we expect local results in higher dimensions to be preserved by use of a center manifold. Note that Corollary 4.2 does not exclude the possibility of "non-banana" resonance regions which do not emanate from the secondary Hopf curve. For example, if the local banana-split horn "partners" connect to form a global banana, we would expect the local parabolic regions to also connect, forming global annuli, projections of tori from the phase $\times$ parameter space. This scenario can be imagined by extending the two p_1/q_1 horns in Figure 1b until they connect, forming a global banana; the global p_0/q_0 region would then likely be an annulus.

We caution our readers that knowing the complete structure of resonance regions for a family of maps does not necessarily mean we have a complete bifurcation classification, even locally in a neighborhood of a nondegenerate Hopf bifurcation point. We do know that all maps on the side of the Hopf bifurcation curve without the invariant circle, including all those on the curve itself, are locally topologically equivalent. We also know that on the side with the invariant curve, the parameter space must be divided at least into the following equivalence classes: the interiors of each resonance region (circles in resonance), each boundary of each resonance region (circles in resonance with saddle-node orbits), and curves "parallel" to the resonance regions along which the corresponding maps restricted to the invariant circle are conjugate to a rigid rotation with an irrational rotation number. What is missing is a guarantee that all the maps in a given resonance region are equivalent. Corollary 2.4 comes close to giving this guarantee: the existence of a *single* attracting/repelling pair of periodic orbits as stated in part 3 of Corollary 2.4 implies that all maps corresponding to parameter values in the interior of a resonance horn and close enough to the tip *are* topologically equivalent.This may not, however, imply that this uniqueness of equivalence classes within a single resonance region can be extended to hold for *all* resonance regions in a fixed neighborhood (not depending on p/q) of a Hopf bifurcation point. This is why in Corollary 2.6, where we make a claim about the shapes of resonance regions "for all p/q sufficiently close to ω_0", we were unable to claim as we did in Theorem 2.3, Corollary 2.4, and Theorem 2.5, that there exists a single pair of period-q orbits inside the corresponding p/q resonance region.

Even if a complete local classification could be established, no such claim could ever be made about the global bananas being the complete bifurcation diagram. Check [ACHM] for example, to see a variety of possible further subdivisions of a single resonance region into further equivalence classes. These further subdivisions are possible, in part, because away from the Hopf curve, as well as near strong resonances, the invariant circle which is born in the Hopf bifurcation may break. This allows non-uniqueness of rotation numbers which in turn allows resonance regions to overlap. Near strong resonances, in fact, they *must* overlap, because of global manifold crossings which imply the existence of an infinite number of periodic orbits for fixed parameter values.

There is an additional number of related questions we have not addressed in this paper: (a) No upper bound is given on the number of resonant Hopf points which may exist on a given two-manifold of period-q points; more than two could certainly exist. We conjecture that Lefschetz index theory could be used to show that the fixed points should generically come in pairs, having indices plus and minus one, respectively. "Mutant" bananas, with 4 tips, for example, could easily be constructed by parameter space surgery on a family having a banana with two tips! (b) Cusp points (saddle-nodes with a higher order degeneracy — not to be confused with cusps at resonant Hopf points) may also appear along the saddle-node boundaries of resonance regions.

They usually appear in pairs, as well, such as on the left-hand side of the subcritical period-5 resonance horn in Figure 6a. Work in progress further describes these pairs of cusps [MP]. (c) Finally, finding examples that would exhibit all schematic scenarios pictured in Figures 5a through 5e remains, to our knowledge, an open problem.

Acknowledgements. We are grateful to R. P. McGehee for helpful discussions and suggestions.

6. Appendix: Proofs.

6.1. Proof of Theorem 2.3. As indicated in subsection 2.2, many of the arguments in this section are adaptations of arguments which Arnold [Ar] uses for $q = 4$. We also note that the symmetry of equation (2) implies that $\mathbf{f}^q(\mathbf{z}) = \mathbf{z}$ is equivalent to $\mathbf{f}(\mathbf{z}) = e^{2\pi ip/q}\mathbf{z}$. The latter equation is easier to use for verifying property 1 of Theorem 2.3, but more difficult to generalize to Corollary 2.4, where the symmetry is not present. So we stick to solving $\mathbf{f}^q(\mathbf{z}) = \mathbf{z}$.

Property 1:

We start with the following lemmas.

LEMMA 6.1. *Assume $q \geq 1$ and*

$$\mathbf{f}(\mathbf{z}) = \boldsymbol{\mu}(\mathbf{z} + A\mathbf{z}^2\overline{\mathbf{z}} + ... + B\overline{\mathbf{z}}^{q-1} + ...) \tag{7}$$

where the omitted terms are all $O(|\mathbf{z}|^{q+1})$, except for those of the form $\mathbf{z}^j\overline{\mathbf{z}}^{j-1}, 3 \leq j \leq \frac{q+1}{2}$ which are $O(|\mathbf{z}|^5)$. Then

$$\mathbf{f}^n(\mathbf{z}) = \boldsymbol{\mu}^n(\mathbf{z} + A(\sum_{k=0}^{n-1}|\boldsymbol{\mu}|^{2k})\mathbf{z}^2\overline{\mathbf{z}} + ... + B(\sum_{k=0}^{n-1}|\boldsymbol{\mu}|^{-2k}\overline{\boldsymbol{\mu}}^{kq})\overline{\mathbf{z}}^{q-1}) + ... \tag{8}$$

where the omitted terms are all $O(|\mathbf{z}|^{q+1})$, except for those of the form $\mathbf{z}^j\overline{\mathbf{z}}^{j-1}, 3 \leq j \leq \frac{q+1}{2}$ which are $O(|\mathbf{z}|^5)$.

Proof. Direct calculation. □

LEMMA 6.2. *Assume the $C^k, k \geq 2$ family of C^∞ maps, $\mathbf{f}_{(\rho,\alpha)}$, is defined by*

$$\mathbf{f}_{(\rho,\alpha)}(\mathbf{z}) = e^{2\pi ip/q}e^{\rho+i\alpha}(\mathbf{z} + A(\rho,\alpha)\mathbf{z}^2\overline{\mathbf{z}} + ... + B(\rho,\alpha)\overline{\mathbf{z}}^{q-1} + ...) \tag{9}$$

where the omitted terms are as in Lemma 6.1. Let $A = A(0,0), B = B(0,0), \mathbf{z} = re^{i\theta}$. Assume $A \neq 0, B \neq 0$, and $q \geq 2$. Then the least-period-q points near $(\rho, \alpha, \mathbf{z}) = (0,0,\mathbf{0})$ are given by the solutions of the equation:

$$\rho + i\alpha + Ar^2 + ... + Br^{q-2}e^{-qi\theta} + ... = 0, r \neq 0 \tag{10}$$

where the θ-independent omitted terms are $O(r^4, \rho^2, \alpha^2, \alpha\rho, \rho r^2, \alpha r^2)$, and all other omitted terms are $O(r^q, \rho r^{q-2}, \alpha r^{q-2})$.

Proof. Period-q points satisfy $\mathbf{f}^q(\mathbf{z}) - \mathbf{z} = \mathbf{0}$. Use Lemma 6.1 to compute $\mathbf{f}^q(\mathbf{z})$, and expand $A(\rho,\alpha), B(\rho,\alpha), \boldsymbol{\mu}^q, \boldsymbol{\mu}^q - 1, \sum_{k=0}^{q-1}|\boldsymbol{\mu}|^{2k}$, and $\sum_{k=0}^{q-1}|\boldsymbol{\mu}|^{-2k}\overline{\boldsymbol{\mu}}^{kq}$, with $\boldsymbol{\mu} = e^{2\pi ip/q}e^{\rho+i\alpha}$ to get power series in ρ and α. Then substitute $\mathbf{z} = re^{i\theta}$ and divide through by $qre^{i\theta}$. (Dividing by r eliminates only the origin, which is a fixed point.) It can be shown (Proposition 3.2 in [CMY] or Theorem 1, Part A in [P2]) that solutions to equation (10) can only have a least period of q or 1. Since period-one points are only at $\mathbf{z} = 0$, then period-q points with $r \neq 0$ must be *least* period-q points. □

Although we cannot solve (10) for the period-q points as a function of the parameters, we can solve for the parameters as a function of the phase variables r and θ. By the implicit function theorem on (10), this is apparently:

$$\rho + i\alpha = -Ar^2 - ... - Br^{q-2}e^{-qi\theta} - ... \tag{11}$$

By choosing r small enough, say less than r_0, we can be sure that Ar^2 dominates all omitted θ-independent terms, and $Br^{q-2}e^{-qi\theta}$ dominates all θ-dependent terms.

For $0 < r \leq r_0, 0 \leq \theta < 2\pi$ equation (11) is an explicit parametrization of the punctured disk which is the least-period-q surface. Adding r=0, corresponding to the resonant Hopf point, fills in the puncture point in the disk. This completes the proof of Property 1.

Property 2:

We now use equation (11) to determine the region in parameter space to which this disk projects. Ignoring the omitted higher order terms, which are the same as for equation (10) in the statement of Lemma 6.2, and, for now, the r^{q-2} term, we get $\rho + i\alpha = -Ar^2 + ...$, or equating real and imaginary parts, respectively,

$$\rho = -A_1 r^2; \alpha = -A_2 r^2 \tag{12}$$

Eliminating r gives:

$$\alpha = \frac{A_2}{A_1}\rho, \frac{\rho}{-A_1} > 0 \tag{13}$$

That is, to the lowest order terms in ρ and α, the parameter values for which period-q points exist trace out a ray in the parameter space from the origin in the direction of $(-A_1, -A_2)$ as r increases from 0.

If we now include the θ-dependent term from equation (11), $Br^{q-2}e^{-qi\theta}$, we see that for a fixed value of r, and letting θ vary from 0 to 2π, a circle in the parameter space is swept out (q times), having center at $(\rho, \alpha) = (-A_1 r^2, -A_2 r^2)$ and radius $|B|r^{q-2}$. When $q \geq 5$, sweeping out all such circles for small r covers a horn-shaped region in the parameter space. See Figure 8 where we have drawn two such circles and the corresponding horn for a resonance region. Since the distance from the origin of these circles varies with r^2 and the width of the horn varies with r^{q-2}, the two sides of the horn are tangent of order $\frac{q-2}{2}$.

This completes the proof of property 2 of Theorem 2.3, but as a heuristic comment, we note that the terms on the right hand side of equation (11), including those not explicitly written, can be separated into θ–independent and θ–dependent terms. If we considered all θ–independent terms, the analogue of equation (12) would be a semi-infinite curve instead a straight ray. This curve we call the "center of the resonance horn." (This would be well defined if the equation were completely in normal form — all non-resonant terms eliminated. This, however, would bring up the question of convergence of an infinite sequence of coordinate changes. Our wish to avoid this technicality is why these comments are merely heuristic.) The center of the resonance horn is still, of course, tangent to the vector $(-A_1, -A_2)$ at the origin. Now adding the $Br^{q-2}e^{-qi\theta}$ term will cause parameter space circles to be swept out as θ varies with r held fixed. The centers of the circles are on the center of the resonance horn. Finally, including the higher order θ–dependent terms will cause the circles which are swept out as θ varies to be slightly deformed. The horn sides are still tangent

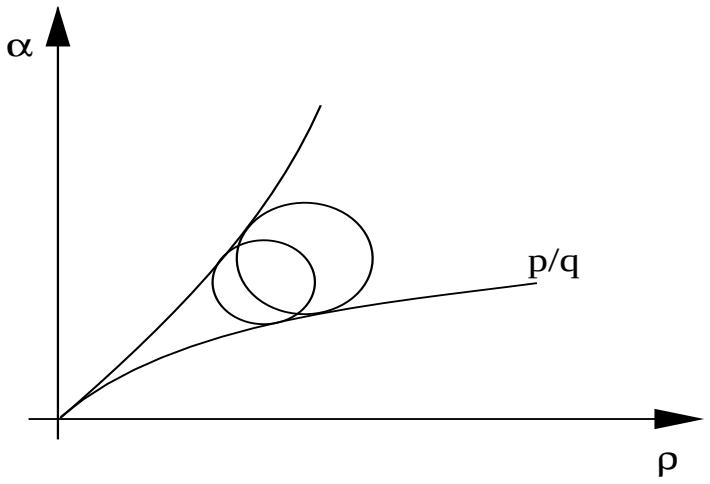

FIG. 8. *"Sweeping out" the resonance horn*

to $(-A_1, -A_2)$ at the origin, and the order of tangency is still $\frac{q-2}{2}$. Thus the only parameter values near $(\rho, \alpha) = (0, 0)$ for which period-q points near $\mathbf{z} = \mathbf{0}$ can exist are inside and on the boundary of the described resonance horn in the parameter space.

Property 3:

(As in Arnold [Ar] for q=4.) From the terms which *do* explicitly appear in equation (11), it is apparent that any point in the interior of the horn lies on exactly two distinct circles, each circle corresponding to a different value of r and having its respective center at $(-A_1 r^2, -A_2 r^2)$. See Figure 8 again. As θ varies from 0 to 2π, each circle is traced out q times (in the negative angular direction). When included, the higher order terms do not qualitatively affect this result. Thus there are q different phase points which correspond to the same parameter value on the circle. In fact, together these q phase points form one complete period-q orbit. Thus each parameter value on the interior of the horn has two distinct period-q orbits for the associated map. That one is a saddle and the other a node is verifiable using techniques similar to those used by Arnold for $q = 4$ (Section 35J in [Ar]).

6.2. Proof of Corollary 2.4. The normal form theorem assures us that the original equation can be brought into the form of equation (1). We would like to make a change of parameters from $\boldsymbol{\mu}$ to (ρ, α) where the relationship between them has already been defined by equation (1). This is possible if the change of parameters, which we will call $\mathbf{h}$, is nonsingular at $\boldsymbol{\mu}_0$. Equivalently, we must have the vectors $\nabla_\mu \alpha(\boldsymbol{\mu}_0)$ and $\nabla_\mu \phi(\boldsymbol{\mu}_0)$ being independent, which we do because we assumed the absence of a parametric degeneracy.

This brings the equation into the form:

$$(14)\quad \mathbf{f}_{(\rho,\alpha)}(\mathbf{z}) = e^{2\pi i p/q} e^{\rho + i\alpha}(\mathbf{z} + A(\mathbf{h}^{-1}(\rho,\alpha))\mathbf{z}^2\overline{\mathbf{z}} + \ldots + B(\mathbf{h}^{-1}(\rho,\alpha))\overline{\mathbf{z}}^{q-1} + \ldots)$$

Now we push through the conclusions and proofs of Theorem 2.3 using the family of equation (14), which is a generalization of our model family of equation (2). The Lemmas used to prove Theorem 2.3 were actually proved already in the more general form of equation (14). Compare equation (14) with equation (6.2) in Lemma 6.2 in

the Appendix, in particular. Since the results of Theorem 2.3 hold for equation (14), both results of the corollary now follow directly the fact that the function $\mathbf{h}^{-1}$ is a nonsingular C^∞ map from the (ρ, α) parameter plane to the $\boldsymbol{\mu}$ parameter plane.

6.3. Proof of item 1 of Theorem 2.5. Rewrite equation (3), replacing ω_0 with $p/q + \alpha_0/2\pi$:

$$\mathbf{f}_{(\rho,\tau)}(\mathbf{z}) = e^{2\pi i p/q} e^{\rho + i(\alpha_0 + c_1\rho + c_2\tau^2)}(\mathbf{z} + A\mathbf{z}^2\overline{\mathbf{z}} + B\overline{\mathbf{z}}^{q-1}) \tag{15}$$

This is the same as the equation for the nondegenerate Hopf bifurcation (equation (2)), but with $\alpha_0 + c_1\rho + c_2\tau^2$ replacing α. Since the nondegenerate analysis was valid for α sufficiently small, the same analysis will hold for $\alpha_0 + c_1\rho + c_2\tau^2$ sufficiently small. We treat α_0 as a third parameter which is small if ω_0 is sufficiently close to p/q.) Therefore we first consider the five dimensional phase $\times$ parameter space, and then obtain the theorem by restricting to an "α_0 = small constant" slice.

The least-period-q set, analogous to equation (10), becomes

$$\rho + i\alpha_0 + c_1\rho + c_2\tau^2 + Ar^2 + \ldots + Br^{q-2}e^{-qi\theta} + \ldots = 0, r \neq 0 \tag{16}$$

Thinking of this complex equation as two scalar equations, we see that the Jacobian with respect to ρ and r^2 at $(r^2, \theta, \rho, \tau, \alpha_0) = (0, \theta, 0, 0, 0)$ is $A_2 - c_1A_1$, which was assumed to be nonzero. So we can solve locally for ρ and r^2 as a function of θ, τ, and α_0. This would seem to indicate the period-q surface is always locally a cylinder: $\theta \in \mathbf{S}^1, \tau \in$ an interval. But the circle swept out as θ varies for a fixed value of r^2 collapses to a point (a fixed point of the map) when $r^2 = 0$, and doesn't exist if $r^2 < 0$. So we must determine the topology of the values of τ which correspond to $r^2 > 0$ and $r^2 = 0$. This is what we proceed to do.

By ignoring the θ dependent terms for now, and eliminating r from equation (16), we obtain an expression analogous to equation (13) for the "center" of our p/q resonance horn to lowest order in the three small parameters ρ, τ, and α_0: $\alpha_0 + c_1\rho + c_2\tau^2 = \frac{A_2}{A_1}\rho, \frac{\rho}{-A_1} > 0$. This is equivalent to:

$$\tau^2 = \frac{A_2 - c_1A_1}{c_2A_1}(\rho - \alpha_0\frac{A_1}{A_2 - c_1A_1}), \frac{\rho}{-A_1} > 0 \tag{17}$$

Treating α_0 as small, nonzero and fixed, we see that there are actually eight cases, all pieces of parabolas, depending on the signs of $\frac{A_2 - c_1A_1}{c_2A_1}$, $\frac{\alpha_0A_1}{A_2 - c_1A_1}$, and A_1. We have sketched the four cases assuming $A_1 < 0$ in Figure 9. The dashed lines are included in the diagram merely for reference — they are the part of the parabola excluded by $\frac{\rho}{-A_1} > 0$, which corresponds to the side of the Hopf curve without the invariant circle. If A_1 were positive, we would get four similar cases, each a reflection across the τ axis of one of the Figure 9 cases. (It might be useful to compare Figure 9a with Figures 3a, $4d_1$, and the horns near D_1 in Figure 1b; Figure 9b with Figures 3b, $4d_2$, and the horns near D_2 in Figure 1b; Figure 9c with Figures 3c, $4d_2$, and the horns near D_2 in Figure 1b.)

We choose an appropriate neighborhood of phase $\times$ (ρ, τ) space by first restricting (ρ, τ, α_0) to a small enough neighborhood of the origin so that the terms explicitly written in equation (16) dominate the (higher order) unwritten terms. We can choose this neighborhood as a cube with sides at $\rho = \pm\overline{\rho}, \tau = \pm\overline{\tau}, \alpha_0 = \pm\overline{\alpha_0}$ by making

small enough choices for $\overline{\rho}, \overline{\tau}$, and $\overline{\alpha_0}$. In cases (a) and (b), we further restrict $\overline{\alpha_0}$, if necessary, so that $\sqrt{|\overline{\alpha_0}/c_2|} < \overline{\tau}/2$. This ensures that in an "$\alpha_0 =$ constant" slice of our three-dimensional space, the banana "tips" on the τ axis are included in the neighborhood.

From Figure 9, it is now apparent that the center curve(s) can be parametrized in the four respective cases (a), (b), (c) and (d) by $\tau \in$

(a) (τ_-, τ_+)
(b) $(-\overline{\tau}, \tau_-) \cup (\tau_+, \overline{\tau})$
(c) $(-\overline{\tau}, \overline{\tau})$
(d) The empty set

where from equation (17), $\tau_\pm = \pm\sqrt{|\alpha_0/c_2|}$.

Reintroducing the θ-dependent terms for $\theta \in [0, 2\pi)$ gives a parametrization of the least-period-q surface as the product of the appropriate set of the above four for τ with the unit circle. The puncture points corresponding to $r^2 = 0$ in cases (a) and (b) are at $\tau_\pm$. This gives us the twice punctured sphere for case (a), the two punctured disks for case (b), the cylinder for case (c), and the empty set for case (d). Including the neglected higher order terms does not change the topology of these sets.

For the projections to the (ρ, τ) parameter space, we fix τ (α_0 is already fixed) and let θ vary from zero to 2π. This traces our a closed curve restricted to $\tau =$ constant in the parameter space. Unless the θ-dependent terms all vanish (including all higher order terms), the closed curve covers a positive length line segment which provides the "thickening" of the respective center lines into regions and establishes the shapes of the respective resonance regions. If the coefficient $B \neq 0$, the length of the line segment varies with r^{q-2} while the distance from the τ axis varies with r^2, establishing the order of tangency at the tips.

For further illustration we have sketched the resonance regions in the three-parameter space (ρ, τ, α_0) in Figure 10 for two distinct cases. The sign of A_1 is assumed to be negative in both cases; the sign of $\frac{A_2 - c_1 A_1}{c_2 A_1}$ is assumed to be positive in the first case, negative in the second. The sign of the third quantity, $\frac{\alpha_0 A_1}{A_2 - c_1 A_1}$ is determined by the sign of α_0, which is one of the parameters in the figure.

6.4. Proof of Corollary 2.6. Restrict to a neighborhood of $(\mathrm{x}_0, \boldsymbol{\mu}_0)$ in phase $\times$ parameter space so that it contains no strongly resonant Hopf points. Choose a p/q with the condition that there is a Hopf point in the restricted neighborhood with eigenvalues $e^{\pm 2\pi i p/q}$. Delete from this neighborhood any of the Hopf points with eigenvalues $e^{\pm 2\pi i r/s}$ with $s < q$. On this deleted, restricted neighborhood, we can change variables to write the equations in the form of equation (1). This defines the functions $\rho(\mu_0)$ and $\phi(\boldsymbol{\mu}_0)$.

We define a change of parameters from $\boldsymbol{\mu}$ to (ρ, τ) where $\rho(\boldsymbol{\mu})$ is defined by equation (1) and τ is a linear variable with respect to the $\boldsymbol{\mu}$ parameter space in a direction perpendicular to $\nabla_\mu \phi(\boldsymbol{\mu}_0)$. This makes $\nabla_\mu \tau(\mu_0)$ and $\nabla_\mu \phi(\boldsymbol{\mu}_0)$ independent vectors and ensures that the parameter change is nonsingular, and therefore a local C^∞ diffeomorphism.

The normal form of equation (1) can now be rewritten as

$$\mathbf{f}_{(\rho,\tau)}(\mathbf{z}) = e^{\rho + i\phi(\rho,\tau)}(\mathbf{z} + A(\rho,\tau)\mathbf{z}^2\overline{\mathbf{z}} + \ldots + B(\rho,\tau)\overline{\mathbf{z}}^{q-1} + \ldots) \tag{18}$$

where the series expansion of ϕ is $\phi(\rho, \tau) = \omega_0 + c_1\rho + c_2\tau^2 +$ higher order terms in ρ and τ. The constant term is determined by the eigenvalues at the bifurcation point

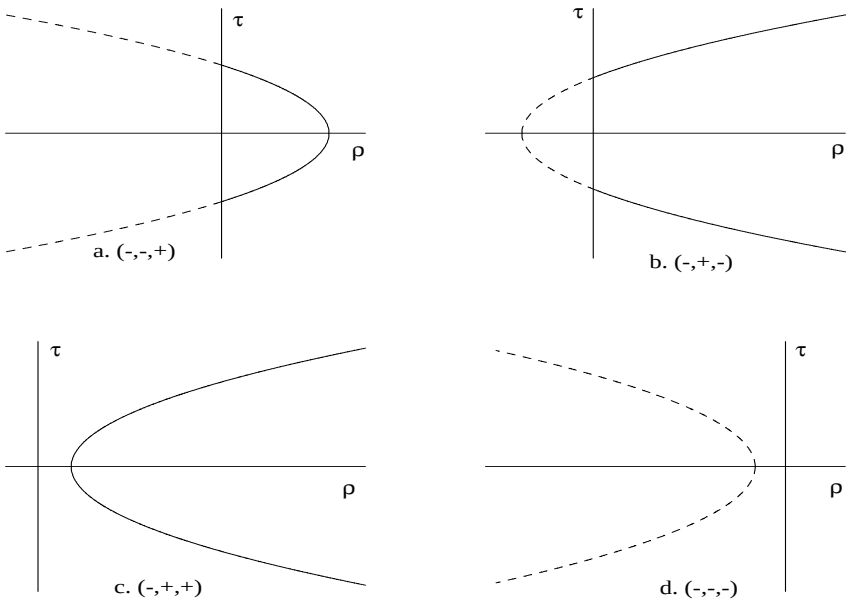

FIG. 9. *"Centers" of resonance regions near a Hopf bifurcation with an angular degeneracy. Labels are for the signs of* A_1, $\frac{A_2 - c_1 A_1}{c_2 A_1}$ *and* $\frac{\alpha_0 A_1}{A_2 - c_1 A_1}$, *respectively.*

μ_0; the τ term is absent because of the angular degeneracy; c_1 is nonzero because we assumed $\nabla_\mu(\alpha(\boldsymbol{\mu}_0)) \neq 0$; c_2 is nonzero because we assumed that $\frac{d^2}{ds^2}\alpha(\boldsymbol{\mu}(s)) \neq 0$. Except for the higher order terms in $\phi(\rho, \tau)$, this family is the same as our model degenerate family of equation (3). The proof of Theorem 2.5 still works for the family in equation (18) because the higher order terms in the expansion of ϕ contribute only to terms already considered as higher order in equation (16).

The fact that the change of parameters between (ρ, τ) and $\boldsymbol{\mu}$ is a local diffeomorphism and the fact that no period-q points can exist arbitrarily close to any of Hopf points deleted from our neighborhood completes the proof.

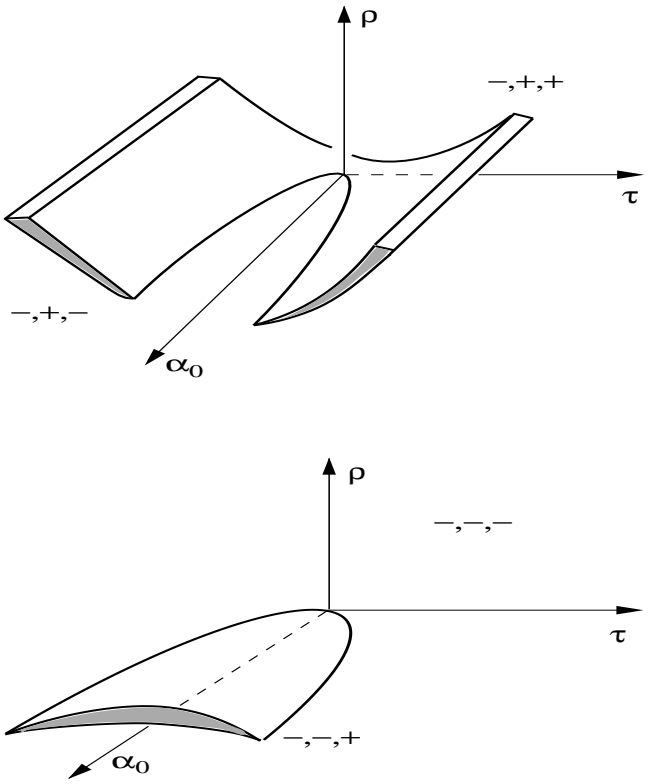

FIG. 10. *Resonance regions in a three parameter space near a Hopf bifurcation with an angular degeneracy. Labels are for the signs of* A_1, $\frac{A_2-c_1A_1}{c_2A_1}$ *and* $\frac{\alpha_0 A_1}{A_2-c_1A_1}$, *respectively.*

REFERENCES

[Ar] V. I. Arnold, *Geometrical Methods in the Theory of Ordinary Differential Equations*, Springer-Verlag, New York, 1983.

[ACHM] D. G. Aronson, M. A. Chory, D. G. Hall, R. P. McGehee, "Bifurcations from an invariant circle for two-parameter families of maps of the plane: a computer assisted study," *Comm. Math. Phys.*, **83**, 303-354, 1983.

[Bo] R. I. Bogdanov,"Versal deformation of a singularity of a vector field in the plane in the case of zero eigenvalues," *Trudy Seminara Imeni I. G. Petrovskogo*, Vol. 2, 23-36, 1976. English translation: *Selecta Math. Sovietica*, Vol. 1, No. 4, 389-421, 1981.

[Ch] A. Chenciner, "Bifurcation de points fixes elliptiques. II. Orbites periodiques et ensembles de Cantor invariants," *Inventiones mathematicae*, **80**, 81-106, 1985.

[CMY] S. N. Chow, J. Mallet-Paret and J. A. Yorke, "A periodic orbit index which is a bifurcation invariant," *Geometric Dynamics (Lecture Notes in Mathematics 1007)*, ed. Palis J., Springer, 109-131, 1983.

[Do] E. J. Doedel, "AUTO: a program for the automatic bifurcation analysis of autonomous systems", *Cong. Num.*, Vol. 30, 265-284, 1981.

[DK] E. J. Doedel and J. P. Kernevez, "AUTO: Software for continuation and bifurcation problems in ordinary differential equations (including the AUTO User Manual)," Report, *Applied mathematics, California Institute of Technology*, 1986.

[Fr] C. E. Frouzakis, "Dynamics of Systems under Control: Quantifying Stability", PhD Thesis, Princeton University, 1992.

[FAK] C. E. Frouzakis, R. A. Adomaitis and I. G. Kevrekidis, "Resonance phenomena in an adaptively-controlled system", *International Journal of Bifurcations and Chaos*, Vol. 1, 83-106, 1991.

[GRC] G. C. Goodwin, P. J. Ramadge and P. E. Caines, *"Discrete-time multivariable adaptive control"*, *IEEE Trans. Automat. Contr.*, **25**, 449-456, 1980.

[GS] G. C. Goodwin and K. S. Sin, *Adaptive Filtering, Prediction, and Control*, Prentice-Hall, Englewood Cliffs, NJ, 1984.

[GH] J. Guckenheimer, and P. Holmes, *Nonlinear Oscillations, Dynamical Systems and Bifurcations of Vector Fields*, Applied Mathematical Sciences, **42**, Springer-Verlag, New York, 1983.

[Jo] J. R. Johnson, "Some properties of a three-parameter family of diffeomorphisms of the plane, near a transcritical Hopf bifurcation," Ph.D. Thesis, University of Minnesota, 1985.

[Mc] R. P. McGehee, personal communications, 1987-88.

[MP] R. P. McGehee and B. B. Peckham, "Resonance surface folds and Arnold flames," in preparation.

[P1] B. B. Peckham,"The Closing of Resonance Horns for Periodically Forced Oscillators," Ph.D. Thesis, University of Minnesota, 1988.

[P2] B. B. Peckham,"The Necessity of the Hopf Bifurcation for Periodically Forced oscillators with closed resonance regions," *Nonlinearity* **(3)** 261-280, 1990.

[Ru] D. Ruelle, *Elements of Differentiable Dynamics and Bifurcation Theory*, Academic Press, Inc., 1989.

[Ta] F. Takens, "Forced oscillations and bifurcations," *Applications of Global Analysis* Communications of the Mathematical Instituet Rijksuniversiteit Utrecht, Vol. 3, 1-59, 1974.